Coordination Chemistry Reviews, 110 (1991) 115–160
Elsevier Science Publishers B.V., Amsterdam

MOLECULAR METALS AND SUPERCONDUCTORS DERIVED FROM METAL COMPLEXES OF 1,3-DITHIOL-2-THIONE-4,5-DITHIOLATE (DMIT)

P. CASSOUX* and L. VALADE

Laboratoire de Chimie de Coordination du CNRS, Unité Propre 8241 liée par conventions à l'Université Paul Sabatier et à l'Institut National Polytechnique de Toulouse, 205 Route de Narbonne, 31077 Toulouse Cedex (France)

H. KOBAYASHI

Department of Chemistry, Faculty of Science, Tokyo University, Funabashi, Chiba, 274 (Japan)

A. KOBAYASHI

Department of Chemistry, Faculty of Science, The University of Tokyo, Hongo 7-3-1, Bunkyo-ku, Tokyo, 113 (Japan)

R. A. CLARK and A. E. UNDERHILL

Department of Chemistry, University of Wales, Bangor, Gwynedd LL57 2UW (U.K.)

(Received 1 November 1990)

CONTENTS

* To whom correspondence should be addressed.

0010-8545/91/$16.10

ABBREVIATIONS

BEDT-TTF	bis(ethylenedithio)tetrathiafulvalene
BPDT-TTF	bis(propylenedithio)tetrathiafulvalene
bpe	2,2′-bipyridinium methylene
bpy	2,2′-bipyridinium
CDW	charge density wave
DBTTF	dibenzotetrathiafulvalene
dcpz	1,4-diethylpyrazinium
DIPSPh$_4$	tetraphenyldithiapyranilidene
DMF	dimethylformamide
dmit	1,3-dithiol-2-thione-4,5-dithiolate
DMSO	dimethylsulphoxide

epy	*N*-ethylpyridinium
EDT-TTF	ethylenedithiotetrathiafulvalene
HMTTeF	hexamethylenetetratellurafulvalene
HOMO	highest occupied molecular orbital
KCP	potassium tetracyanoplatinate, partially halogenated
LUMO	lowest unoccupied molecular orbital
$[M(bdt)_2]$	bisdithiolene metal complexes
mnt	maleonitriledithiolate
SDW	spin density wave
TCNQ	7,7′,8,8′-tetracyano-*p*-quinodimethane
TMTSF	tetramethyltetraselenafulvalene
TMTTF	tetramethyltetrathiafulvalene
TSF	1,4,5,8-tetraselenafulvalene
TSeT	tetraselenatetracene
TTF	1,4,5,8-tetrathiafulvalene
TTT	tetrathiatetracene

A. INTRODUCTION

Metal complexes of sulphur ligands have been of interest for many years because of their applications in analytical chemistry, catalysis and their relevance to bio-inorganic systems [1–3]. A more recent development has been concerned with the unusual solid state properties sometimes found for these compounds. Currently there is much interest in the search for new and improved synthetic molecular metals [4] and many of these are based on planar organic donor molecules which contain sulphur or selenium heteroatoms [5,6]. In some cases it is possible to synthesize ligand systems which possess many of the structural and electronic properties of fragments of these sulphur- or selenium-containing donor organic molecules. When these ligands are combined with suitable metal ions to form planar anions, molecular metals and superconductors may be formed. The principal interest in the metal complexes of the dmit ligand is the structural similarity with the organic donor molecule, BEDT-TTF (Fig. 1) with its proven ability to form both molecular metals and molecular superconductors [4–6].

The first molecular metals based on metal complexes were prepared in the mid-1800s, but it was not until the late-1960s that the unusual solid state properties of these materials were studied [7,8]. In the 1960s, research workers found that solid state interactions resulted in unusual properties for complexes such as $K_2[Pt(CN)_4]Br_{0.3} \cdot 3H_2O$ (KCP) [9]. This material, for example, exhibited essential one-dimensional metal-like characteristics resulting from the closed approach of the central metal atoms along one crystal axis, thus allowing overlap of the metal d_{z^2} orbitals. However, it was found that only a limited number of compounds could be formed based on $[Pt(CN)_4]$ or $[Pt(C_2O_4)_2]$ anions, all of which underwent a metal-

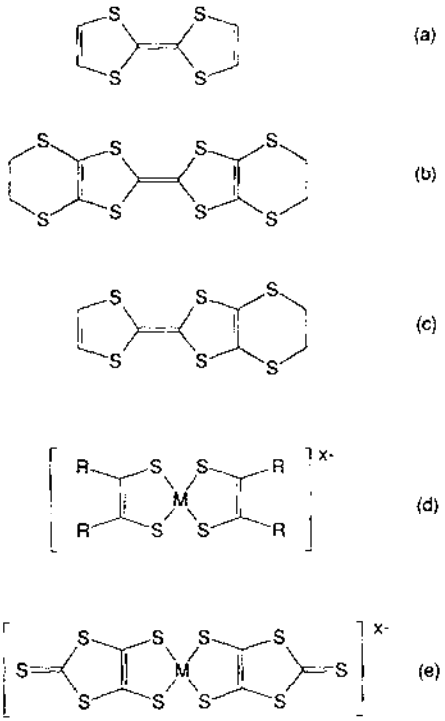

Fig. 1. (a) TTF; (b) BEDT-TTF; (c) EDT-TTF; (d) $[M(bdt)_2]$; (e) $[M(dmit)_2]$.

to-semiconductor transition above 70 K [10]. This contrasts with the many organic compounds which are low-temperature superconductors, either under pressure or at ambient pressure [4–6]. All these organic superconductors are based on molecules derived from the TTF molecule (Fig. 1) and originate from the first organic metal, TTF · TCNQ [11]. In these systems, metallic properties arise from the overlap of the partly delocalized π molecular orbitals of the molecules.

Consequently, considerable effort has been put into incorporating the structural features of the organic metals into the ligands present in metal complexes in order to increase the interactions of the molecules through the ligand systems. Since the large sulphur atomic orbitals play an important role in promoting effective intermolecular overlap in the organic metals, a high degree of peripheral sulphur has been incorporated, where possible, in these ligands.

As mentioned previously, the first organic metals were based on the donor, TTF. Metal bisdithiolene complexes, $[M(bdt)_2]$ or $[M(S_2C_2R_2)_2]$ (Fig. 1), particularly those in which R is CF_3 [12] or CN [13], are structurally analogous to the TTF molecule and have been extensively studied and used for the preparation of fractional oxidation state complexes or π donor–acceptor compounds. $(H_3O)_{0.33}Li_{0.82}[Pt(S_2C_2(CN)_2] \cdot 1.67H_2O$ was the first transition metal complex of

the metal bisdithiolene series in which metal-like behaviour was not related to the presence of a TTF-like donor molecule but due to inter-molecular interaction of the metal complex anions [13]. However, as for its KCP forbear, this complex also underwent a metal-to-semiconductor transition at about 270 K. The number of new molecular metals that could be prepared based on metal bisdithiolene complexes, has been found to be rather limited.

The establishment of the metallic state in a molecular system requires:

(a) effective inter-molecular orbital overlap to establish a delocalized band structure; and

(b) partial occupation by electrons of the delocalized band structure.

It is also well known that one-dimensional (1D) metals are subject to the Peierls instability [14], which converts the metal to a semiconductor by means of an appropriate lattice distortion. It has been suggested [15] that increasing interstack interactions can suppress the Peierls instability and preserve the metallic state down to low temperatures. Thus the organic donor BEDT-TTF is an improvement on the original donor, TTF, and the dmit ligand (1,3-dithiol-2-thione-4,5-dithiolate; Fig. 1) is an improvement on the simple dithiolene ligand. The synthesis of the dmit ligand was first reported in 1975 by Steimecke et al. [16] and the preparation of the nickel complex as the tetraethylammonium salt in 1979 [17] has initiated a series of papers over the last decade concerned with using this ligand to generate metal complexes with unusual electronic properties.

The $[M(dmit)_2]$ species (Fig. 1) can exist as the dianion, the monoanion or the neutral complex. In the dianion and the neutral complex, the HOMO will contain a pair of electrons and therefore any delocalized band formed by overlap of the HOMO on adjacent molecules will be completely full, resulting in semiconducting properties. However, the monoanion will contain a single electron in the HOMO and therefore, in this case, the resulting delocalized band would be expected to be half full. Such a system would be very susceptible to the Peierls instability [14], resulting in the formation of dimers and of a filled band, and consequently in semiconducting properties.

In the solid state, however, provided that there are interactions between the molecules, the electronic charge per molecule can be non-integral. With "closed-shell" cations, a rational fraction of charge per anion would be expected to depend upon the stoichiometry of the compound. For example, in $[Me_4N][Ni(dmit)_2]_2$, the charge per anion is $-1/2$. However, for "open-shell" organic anions the situation is potentially much more complicated. It is well known that for organic charge transfer salts formed between open-shell donors and acceptors, the extent of charge transfer varies and is dependent in part upon the relative values of the ionization energy of the donor and the electron affinity of the acceptor [18]. Molecular metals are observed when a non-integral amount of charge per molecule is transferred from the donor to the acceptor. Thus, although the stoichiometry of TTF · TCNQ is 1:1, the amount of charge transferred per molecule from the TTF to the TCNQ is 0.59 [11].

Since the literature now offers over one hundred papers dedicated to the dmit system, a review of this system is overdue. Here we present a review of the current state of research into the metal–dmit complexes with reference to the central metal ion and the variety of counter cations used.

B. PREPARATION OF THE LIGAND DMIT

In 1975, Steimecke et al. reported that treating carbon disulphide with an alkali metal in the presence of DMF (dimethylformamide) produced a mixture of the ligand dmit as the dianion salt, isotrithione-dithiolate (or 1,3-dithiol-2-thione-4,5-dithiolate) and the dianion salt trithiocarbonate (Scheme 1) [16].

A convenient way to prepare and protect the reactive ligand is by stabilizing it as the zinc complex. To do this, the reaction mixture is treated with $ZnCl_2$ in a NH_3,H_2O/MeOH solution, then with tetraalkyl ammonium bromide (R_4N; R = ethyl or butyl) in methanol to give, exclusively, a precipitate of $(R_4N)_2[Zn(dmit)_2]$ since the R_4N salt of the other product is soluble. Treatment of $(R_4N)_2[Zn(dmit)_2]$ with

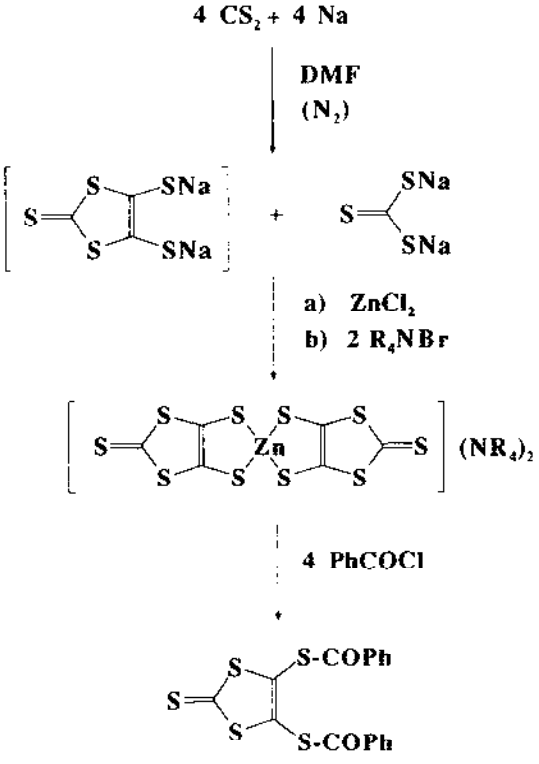

Scheme 1.

benzoyl chloride in acetone gives the thioester product 4,5-bis(benzoylthio)-1,3-dithiol-2-thione, which can be conveniently stored as a precursor for further work.

This method of preparation forms the basis of all work in this area. The ligand itself can be isolated as the highly reactive sodium salt using standard Schlenk techniques [19]. Most preparations within this field involve as a starting material one of the tetraalkyl ammonium salts of $[M(dmit)_2]^{2-}$ since they are amongst the most easily prepared and purified [17].

C. $[Ni(dmit)_2]$ COMPOUNDS

The $[Ni(dmit)_2]$ compounds are the most widely studied of all the dmit compounds. This is a reflection of the fact that they have yielded more examples of molecular metals or superconductors than the complexes of other metals, such as Pd or Pt.

(i) Neutral $[Ni(dmit)_2]$

The neutral $[Ni(dmit)_2]$ compound was obtained as plate-like crystals as a minority product during the preparation of $TTF[Ni(dmit)_2]_2$ [20]. Within the crystal structure the molecules stack along the [010] direction, making an angle with the normal to the molecular mean plane of 48° [20]. Within the stack, the Ni–Ni spacing is 5.302 Å and the plane-to-plane distance 3.562 Å. There are short S ··· S contacts between adjacent stacks involving the thioketone sulphur atom. The low conductivity, 3.5×10^{-3} S cm^{-1} reflects the lack of a fractional oxidation state for the compound [20].

(ii) $[Ni(dmit)_2]$ salts of "open-shell" organic cations

A variety of salts of "open-shell" donor cations with the $[Ni(dmit)_2]$ anion has been prepared [21–42] and are listed in Table 1.

It can be seen from Table 1 that a variety of stoichiometries is obtained, depending upon the open-shell cation used. It is not clear why such a variety of stoichiometries is obtained or whether, by an appropriate choice of experimental conditions, different stoichiometries could be obtained. However, these differences in stoichiometry make any meaningful comparison of the compounds impossible. The replacement of sulphur by selenium has changed the stoichiometry from $TTF[Ni(dmit)_2]_2$ to $TSF[Ni(dmit)_2]_3$. Such changes in stoichiometry are obviously accompanied by large structural differences and these will account for the differences in solid state properties listed in Table 1. However, it is significant that, in spite of the differences in stoichiometry and structure, all the compounds exhibit moderate or high electrical conductivities at room temperature.

As can be seen from Table 1, the only compound which behaves like an organic

TABLE 1

[Ni(dmit)$_2$] salts with "open shell" organic cations

Compound	σ_{RT}/S cm^{-1} [a]	Crystal structure ref.	Other ref.
TTF[Ni(dmit)$_2$]$_2$	$\approx$300 (m)[b]	21	22 32
TSF[Ni(dmit)$_2$]$_3$	$\approx$4 (sc)[b]	33	
α-(EDT-TTF)[Ni(dmit)$_2$]	100 (m)[b]	34	
β-(EDT-TTF)[Ni(dmit)$_2$]	10^{-2}(sc)[b]	34	
DBTTF[Ni(dmit)$_2$]	$\approx$300 (unknown)	35	25,36
TMTTF[Ni(dmit)$_2$]$_y$ ($1<y<2$)	$\approx 10^{-4}$ (sc)		37
TMTSF[Ni(dmit)$_2$]	$\approx$300 (sc)[b]	38	37
α-(BPDT-TTF)[Ni(dmit)$_2$]$_2$	$\approx$10 (sc)[b]	39	
BEDT-TTF[Ni(dmit)$_2$]	$\approx 2\times10^{-3}$ (sc)[b]	40	36,37
(bpy)$_3$[Ni(dmit)$_2$]$_5$	$\approx$7.5 (unknown)		27
(bpe)[Ni(dmit)$_2$]$_2$	$\approx 6\times10^{-3}$ (unknown)		27
(DIPSPh$_4$)$_3$[Ni(dmit)$_2$]	$\approx 10^{-1}$ (sc)		27
(DIPSPh$_4$)[Ni(dmit)$_2$]	$<10^{-5}$ (sc)[b]		41
(depz)$_{0.3-0.35}$[Ni(dmit)$_2$]	$\approx 10^{-3}$ (sc)		42

[a] m = metal-like conductivity; sc = semiconductor-like conductivity.
[b] Measurement on single crystal, remainder measured on compressed pellet.

metal and maintains this state to low temperature (1.5 K) is the salt with TTF. Consequently, the study of this system has somewhat dominated the field. An interesting series of compounds has been prepared with the donors bpy, bpe and depz but these systems have not, as yet, produced metals [27].

(a) TTF[Ni(dmit)$_2$]$_2$

(1) Synthesis of TTF[Ni(dmit)$_2$]$_2$. Single crystals of TTF[Ni(dmit)$_2$]$_2$, which was the first molecular superconductor containing a transition metal complex, were formed by slow inter-diffusion of solutions of (TTF)$_3$(BF$_4$)$_2$ and (n-Bu$_4$N)[Ni(dmit)$_2$], at 30–46°C, using a three-compartment H-shaped tube [21]. This technique led to the formation of a majority product, TTF[Ni(dmit)$_2$]$_2$, and of a minority product, [Ni(dmit)$_2$], which were differentiated by X-ray diffraction. Electrochemically synthesized crystals appeared to be inferior in size and quality [22].

(2) Structure of TTF[Ni(dmit)$_2$]$_2$. Essentially, the structure of TTF[Ni(dmit)$_2$]$_2$ may be described as segregated stacks of donor and acceptor molecules along the b axis (Fig. 2). Both are planar, although the [Ni(dmit)$_2$] anions are slightly bent out of the plane by $\approx$4° [22]. The intrastack spacing is 3.73 Å, but due to both molecules being tilted out of the (010) plane, the mean interplanar spacings are slightly different ([Ni(dmit)$_2$] tilt = 18°, spacing $\sim$3.55 Å, TTF tilt = 12°, spacing $\sim$3.65 Å). Interest-

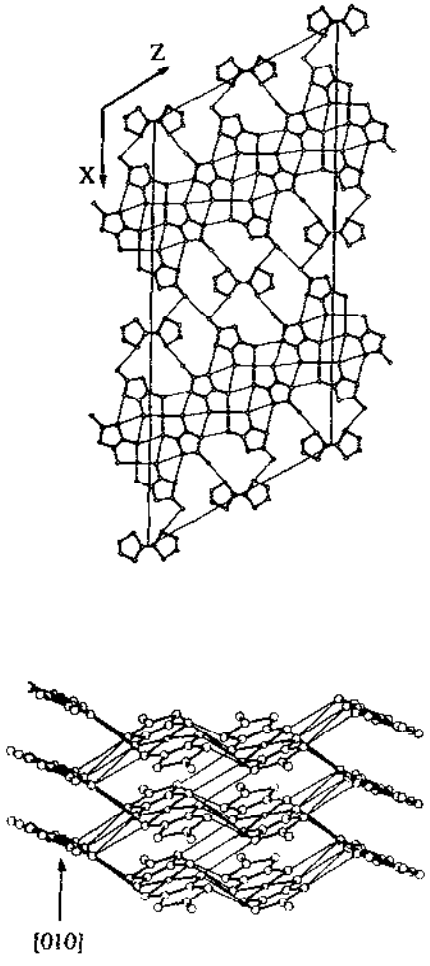

Fig. 2. The "3D" crystal structure of $TTF[Ni(dmit)_2]_2$. *Thin lines* indicate S ··· S distances shorter than 3.70 Å.

ingly, the large separation between $[Ni(dmit)_2]$ anions within a stack leads to S ··· S distances larger than the sum of the corresponding van der Waals radii (3.70 Å). There is, however, a large number of intermolecular interstack interactions, which have distances much shorter than the corresponding van der Waals radii. These interactions occur between $[Ni(dmit)_2]$ anions positioned in adjacent stacks but at different levels relative to (010) and consequently a two-dimensional network of $[Ni(dmit)_2]$ interactions along both the *b* and *c* directions may be considered. The TTF cations are also involved in short S ··· S contacts with the thione moieties of the $[Ni(dmit)_2]$ anions. This could extend further the S ··· S contacts along the *a* axis so that, overall, a three-dimensional network would appear to be present.

It has been suggested that, on the basis of simple tight binding band calculations involving only the LUMO bands, the system would appear to be essentially a regular 1-D chain system, with the overlap integrals being small in all directions besides those parallel to [010] [25]. This is due to the location of the nodal plane of the LUMO of the neutral molecule on the central Ni atom, which makes the transverse intermolecular overlap integral small. Since we would not expect a high degree of interaction parallel to [010], and since this system could appear to be a quasi-3D system which exhibits metal-like conductivity, this result is in contrast to other evidence. It was proposed that the unusual electrical conductivity of this sample could be explained by the fact that it is a "multi-band Fermi surface system" which might be the main difference with the other 1-D chain systems [25]. Hence, it may show that charge density wave and spin density wave transitions may be suppressed even in a strongly 1-D system. It has been more recently proposed, on the basis of more detailed calculations including also the HOMO bands, that both the LUMO and HOMO bands of the $Ni(dmit)_2$ acceptor molecules are partially filled and also that the multi-band Fermi surface $TTF[Ni(dmit)_2]_2$ system exhibits some two-dimensional character at the Γ point of the Brillouin zone [43].

(3) Electrical conductivity of $TTF[Ni(dmit)_2]_2$. The room temperature electrical conductivity measured along the needle axis of the single crystal (i.e. parallel to the [010] axis) was found to be $\sim 300\ S\ cm^{-1}$. The temperature dependence of the conductivity was studied, the crystal behaving like a metal down to 4 K, at which point the conductivity was $\sim 1.5 \times 10^5\ S\ cm^{-1}$ (Fig. 3) [21]. Further measurements indicated that $TTF[Ni(dmit)_2]_2$ remains metallic down to 1.5 K [44] and is not superconducting above 47 mK [23]. A study of the pressure-dependence of the conductivity at low temperature showed that it exhibited superconductivity with $T_c = 1.62$ K at 7 kbar (Fig. 4) [24].

Low-field ESR studies have shown that T_c decreases with decreasing pressure down to 1.29 K at 3 kbar [30]. This was later confirmed by conductivity measurements under pressure [32]. The effect of pressure on T_c is therefore opposite to that observed in all other organic molecular superconductors of the TMTSF and BEDT-TTF families [45,46]. The complete, unusual, temperature-pressure phase diagram of $TTF[Ni(dmit)_2]_2$ has been recently determined [44,47]. Increasing pressure induces various, successive, electronic phase transitions from a high-temperature metallic state to semi-metallic, semiconducting, and re-entrant superconducting states. These results suggest that superconductivity co-exists with a high-temperature CDW instability and is in weak competition with low-temperature CDW fluctuations, with the instability and fluctuations affecting different parts of the Fermi surface [43]. In fact, ambient-pressure X-ray scattering studies provide experimental evidence for CDW instabilities in this compound [48,49].

^1H NMR relaxation data, low- and high-resolution ^{13}C NMR studies on $TTF[Ni(dmit)_2]_2$ have also been reported [31,50,51]. The results confirm the occur-

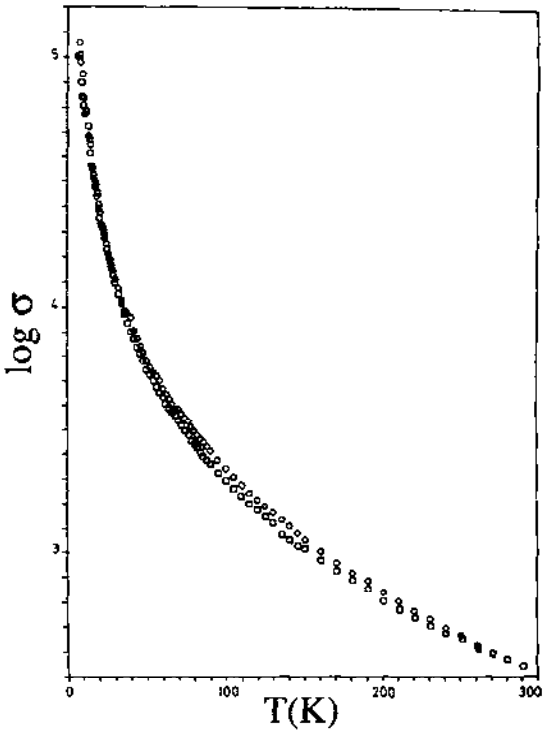

Fig. 3. Log conductivity vs. temperature for a crystal of TTF[Ni(dmit)$_2$]$_2$ (○ = cooling; □ = subsequent warming).

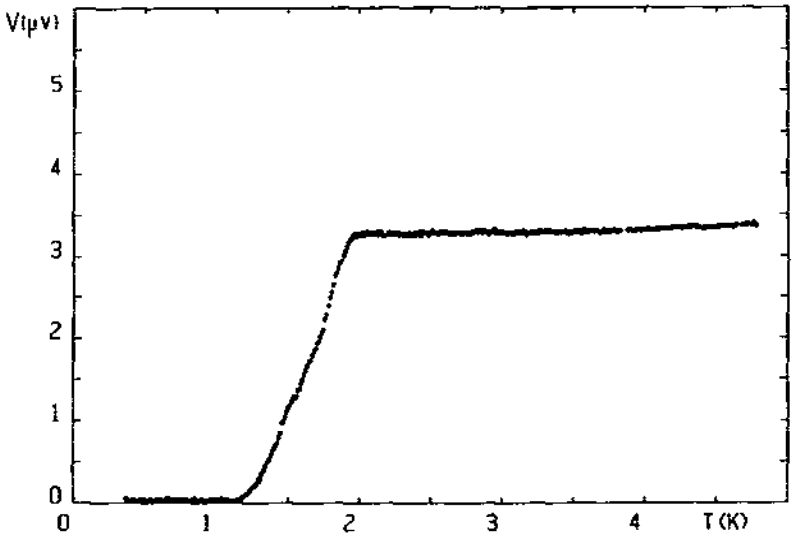

Fig. 4. Superconducting transition of TTF[Ni(dmit)$_2$]$_2$ at 7 kbar. $I = 67.5$ μA; $T_c = 1.62$ K; $\Delta T_c = 0.57$ K.

rence of both HOMO and LUMO conduction bands and suggest that the CDW effects above 160 K are associated with the LUMO bands. It is also interesting to note that thermopower studies have shown that, at temperatures below 77 K, there is an inversion in the sign of the carriers, holes becoming the dominant carriers [52]. Unusual magnetoresistance data have also been reported for $TTF[Ni(dmit)_2]_2$ and indicate a low anisotropy [29].

It is known that the onset of a CDW state usually induces a Peierls metal-to-insulator transition in a molecular low-dimensional conductor and metal-like conductivity is suppressed. This is not observed in $TTF[Ni(dmit)_2]_2$, which remains metallic at ambient pressure down to low temperatures. This could be explained by the multiconduction band system of the $Ni(dmit)_2$ stacks consisting of HOMO and LUMO bands. The CDW instability could open a gap in only some of these bands, leaving the other bands unaffected, so that some metallic bands will remain. Consequently, the remaining carriers at low temperatures (holes) could come from these metallic bands, and also from TTF bands as indicated by ^1H NMR data, which did not reveal any gap opening in the electronic excitation of the TTF stacks down to 1.5 K [31].

(b) (EDT-TTF)[Ni(dmit)$_2$]

EDT-TTF (see Fig. 1) is a hybrid between TTF and BEDT-TTF molecules. Two distinct crystal forms (α, β) were obtained by electrocrystallization in various solvents [34].

(1) α-(EDT-TTF)[Ni(dmit)$_2$]. An acetronitrile solution gave the α form as black hexagonal plates. The planar $[Ni(dmit)_2]$ molecules form a uniform column along the *b* axis with the interplanar distance of 3.52 Å. The asymmetric EDT-TTF molecules stack alternately along the [110] direction. The interplanar distances are 3.62 and 3.61 Å [34].

The room-temperature conductivity of the α form is about 100 S cm^{-1}. The electrical resistivity exhibits a monotonous decrease down to 20 K, whereupon the resistivity then begins to increase and shows a peak around 14 K. It then decreases with decreasing temperature, as for a metal (Fig. 5). No structural change was observed around 15 K [34(c)]. The reflectance spectra of the α form suggests a small anisotropy of the electronic structure in the *ab* plane. The band structure consists of two quasi one-dimensional metallic bands, each of which is associated with the $Ni(dmit)_2$ and EDT-TTF stacks. Owing to the two pairs of "warped" planes of Fermi surfaces which are not completely nested by a single modulation wave vector, the metallic state of the α-(EDT-TTF)$[Ni(dmit)_2]$ seems to be stabilized.

(2) β-(EDT-TTF)[Ni(dmit)$_2$]. A 1,2-dichloroethane–acetonitrile (1:3) solution afforded mainly the β form as black thin plates. The β form has a mixed-stacking

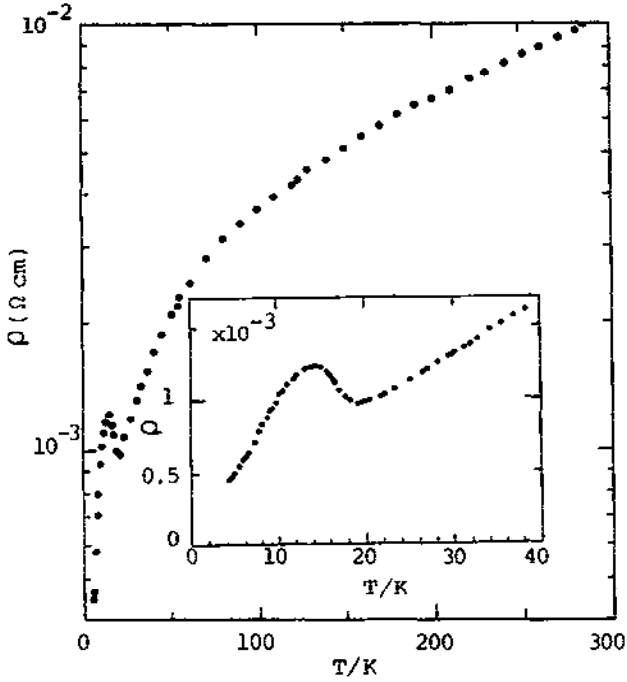

Fig. 5. Electrical resistivity of α-(EDT-TTF)[Ni(dmit)$_2$].

structure. The room temperature conductivity is 10^{-2} S cm^{-1} and temperature dependence is that of a semi-conductor.

(c) α-(BPDT-TTF)[Ni(dmit)$_2$]$_2$

The structure of α-(BPDT-TTF)[Ni(dmit)$_2$]$_2$ shows segregated uniform columns of donor and acceptor molecules [39], the two Ni(dmit)$_2$ columns forming a paired chain. The room-temperature conductivity is 5–10 S cm^{-1} and at 120 K, a narrow-gap semiconductor-to-insulator transition is observed. The crystal structure determined at 96 K is almost identical with that determined at room temperature, except for the enhancement of the S ··· S transverse interaction in the Ni(dmit)$_2$ paired chain.

(d) (DIPSPh$_4$)$_y$[Ni(dmit)$_2$] (y=3, 1)

Needle-shaped crystals of (DIPSPh$_4$)$_3$[Ni(dmit)$_2$] have been obtained by Zhu et al. [27] by electrochemical oxidation of DIPSPh$_4$ in a dichloromethane solution containing (n-Bu$_4$N)$_2$[Ni(dmit)$_2$]. The conductivity along the needle axis is 1–10 S cm^{-1} and temperature dependence is that of a semi-conductor (E_a=0.15 eV). Using a similar electrochemical method, but starting with the monovalent salt (n-Bu$_4$N)[Ni(dmit)$_2$], instead of the divalent salt (n-Bu$_4$N)$_2$[Ni(dmit)$_2$], blue parallelepi-

pedic crystals of a different phase, the 1:1 adduct $(DIPSPh_4)[Ni(dmit)_2]$, have been obtained and characterized by an X-ray structural determination [41]. The structure is characterized by a loose stacking (>10 Å) of $Ni(dmit)_2$ units along [001], with no strong intermolecular interaction, consistent with the low electrical conductivity ($<10^{-5}$ S cm^{-1}). Surprisingly, analysis of the results of a detailed single-crystal EPR study indicates that dipolar spin–spin interaction takes place in this highly electron-correlated semiconducting system with complete charge transfer between the donor $DIPSPh_4$ and the acceptor $Ni(dmit)_2$ [41].

(iii) [Ni(dmit)$_2$] salts with "closed-shell" organic cations

A series of closed-shell organic cation salts of $[Ni(dmit)_2]^{n-}$ have been prepared [17,20,43,53–76] and are listed in Table 2. The tetraethylammonium salt was originally prepared by Steimecke et al. [17] in order to determine the crystal structure

TABLE 2

$[Ni(dmit)_2]$ salts with "closed shell" organic cations

Compound	σ_{RT}/S cm^{-1} [a]	Crystal structure ref.	Other ref.
$(Me_4N)[Ni(dmit)_2]$		53	
$(Me_4N)[Ni(dmit)_2]_2$	≈60 (m to 100 K, sm below 100 K)[b]	54	43,55–58
$(Et_4N)[Ni(dmit)_2]$	$\approx 10^{-5}$ (sc)[b]	58	53,59–62
$(Et_4N)[Ni(dmit)_2]_2$	4.5×10^{-2} (sc)[b]	63	53,59
$(Pr_4N)[Ni(dmit)_2]$		53	61
$(n\text{-}Bu_4N)_2[Ni(dmit)_2]$		64	17
$(n\text{-}Bu_4N)[Ni(dmit)_2]$	3×10^{-8}	65,66	17,26,58
$(n\text{-}Bu_4N)_{0.29}[Ni(dmit)_2]$	≈10 (sc)[b]	20	
$\alpha\text{-}(Et_2Me_2N)[Ni(dmit)_2]_2$	20–100 (m to 1.5 K)[b]	67	68
$\beta\text{-}(Et_2Me_2N)[Ni(dmit)_2]_2$	3 (sc)[b]	68	
$(EtMe_3N)[Ni(dmit)_2]_2$	0.4 (sc)	68	
$(Me_4P)[Ni(dmit)_2]_2$	0.6 (sc)	68	
$(Me_4As)[Ni(dmit)_2]_2$	0.1 (sc)	68	
$[Me_3S(O)][Ni(dmit)_2]_2$	1 (sc)	68	
$(HMe_3N)[Ni(dmit)_2]_2$	300 ± 200 (m to 120 K, sc to 15 K, m below 15 K)	69	70,71
$(H_4N)_x[Ni(dmit)_2]$	0.3 (sc)–50 (m)[b]	72	73
$(Ph_4As)[Ni(dmit)_2]_4$	10–15 (sc)[b]	74	
$[Me_2(C_nH_{2n+1})_2N][Ni(dmit)_2]_2$[c]	Insulating		75,76

[a] m = metal-like conductivity; sm = semi-metal-like conductivity; sc = semiconductor-like conductivity.

[b] Measurement on single crystal, remainder measured on compressed pellet.

[c] n = 10, 12, 14, 16, 18, 22.

of the $(Et_4N)_2[Ni(dmit)_2]$ complex [64]. Tetraalkylammonium salts have proved to be useful starting materials for the preparation of other compounds because of the ease of recrystallization of the salt and its solubility in common solvents.

The salts can be obtained with different formal negative charges associated with the anion. These are:

(a) dianion salts, $[Ni(dmit)_2]^{2-}$: this is the charge on the anion as prepared;

(b) monoanion salts, $[Ni(dmit)_2]^{-}$: the mono-anion salt can be prepared by I_2 oxidation of the dianion salt; and

(c) fractional oxidation state salts, $[Ni(dmit)_2]^{x-}$: they are generally prepared by electrocrystallization techniques.

(a) Dianion salts

$(n\text{-}Bu_4N)_2[Ni(dmit)_2]$ is obtained as small green transparent crystals, although larger crystals appear black and opaque. The crystal structure contains columns of planar $[Ni(dmit)_2]$ dianions [64]. However, there are no S ··· S contacts shorter than the van der Waals distances. $(Et_4N)_2[Ni(dmit)_2]$ has also been reported [58].

(b) Mono-anion salts

$[Et_4N][Ni(dmit)_2]$ was prepared by iodine oxidation of the dianion salt [58]. The quasi-planar $[Ni(dmit)_2]$ anions stack along the a axis with alternating Ni–Ni distances of 4.163 and 4.243 Å. The chains are well separated with the shortest S ··· S distances of 3.8 Å, whereas the face-to-face distances along the stack are 3.5 and 3.7 Å. The room-temperature conductivity (two-probe) is 4×10^{-5} S cm^{-1} with $\sigma_{\parallel}/\sigma_{\perp}>100$. The temperature-dependence of the conductivities does not follow the $\log\sigma\propto T^{-1}$ commonly found for semiconductors. However, it does follow a $\log\sigma\propto T^{-1/2}$ over seven decades of conductivity. This temperature-dependence has been explained on the basis that the system is effectively disordered due to large thermal vibration of the anions resulting in electron localization [60].

Two phases of $(n\text{-}Bu_4N)[Ni(dmit)_2]$ have been described [17,26,58,65,66]. The first one is obtained by iodine oxidation of the dianion salt [17] and crystallizes in the space group $P2_1/c$ [65]. There is a significant shortening of the Ni–S bond in the mono-anion salt compared with the dianion. There is no stacking of the $Ni(dmit)_2$ units, but strong S ··· S contacts (3.402 and 3.546 Å) are observed [65]. The conductivity has been reported to be 3×10^{-8} S cm^{-1} [58]. Another $(n\text{-}Bu_4N)[Ni(dmit)_2]$ phase, which crystallizes in the space group $P\bar{1}$ [66], has been directly obtained from the ligand [26]. The packing arrangement of this phase is completely different from that of the previous phase: there is stacking of the $Ni(dmit)_2$ units, but no strong S ··· S contacts are observed.

(c) Fractional oxidation state salts

(1) $(Me_4N)[Ni(dmit)_2]_2$. This is an interesting salt of a redox active metal complex anion. It is the first salt with a "spectator" "closed shell" donor cation to behave like

a metal down to 100 K, and even more importantly, to undergo a superconducting transition under pressure [54,55].

As with other conducting $[Ni(dmit)_2]$ salts, good quality crystals were obtained by electrocrystallization from an acetonitrile solution of $(Me_4N)[Ni(dmit)_2]$ and $(Me_4N)ClO_4$ with a constant current of 0.6 μA.

In $(Me_4N)[Ni(dmit)_2]_2$, the $[Ni(dmit)_2]$ anions, which are almost planar, are stacked along [110], forming an apparent 1-D four-fold structure (Fig. 6) [54]. However, because the lattice is C-centred, the real repeat unit contains two anions and the tetramethylammonium cations are ordered within this lattice. An important feature of the lattice is the close similarity of the two independent interplanar distances (3.58 and 3.53 Å). The two modes of overlap along the molecular stacks are shown in Fig. 7. Short S ··· S contacts, with distances less than the van der Waals radii, are found to exist between adjacent stacks of $[Ni(dmit)_2]$ anions. Consequently, the conduction path may be considered to be facilitated by inter-molecular interstack interactions. The first reported tight-binding band calculation shows the existence of two pairs of open Fermi surfaces corresponding to the two different directions ([110], [1$\bar{1}$0]), which is in good agreement with the result of the analysis of the optical reflection [57]. Subsequent tight-binding band calculation including the HOMO as well as the LUMO of the $Ni(dmit)_2$ molecules shows that, because of the slight dimerization observed in $(Me_4N)[Ni(dmit)_2]_2$, only the LUMO band is partially filled, whereas both the HOMO and LUMO bands were found to be partially filled in $TTF[Ni(dmit)_2]_2$ [43].

The room-temperature conductivity of $(Me_4N)[Ni(dmit)_2]_2$ is about 50 S cm^{-1} along two directions parallel to the (001) plane, and 10^{-2} S cm^{-1} along the direction perpendicular to this plane. The sample dependence of the resistivity behaviour is large. Some samples are metallic down to about 10 K, below which the resistivity becomes activated. However, there are many crystals exhibiting a resistivity jump around 100 K. In the latter cases, upon cooling, the crystal metallic behaviour is observed down to about 100 K whereupon the conductivity falls sharply. Between 100 and 30 K, the conductivity remains roughly constant. A strong hysteresis is

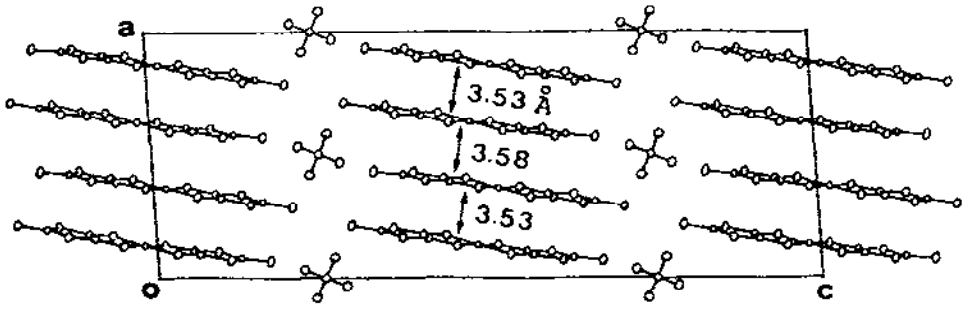

Fig. 6. Crystal structure of $(Me_4N)[Ni(dmit)_2]_2$.

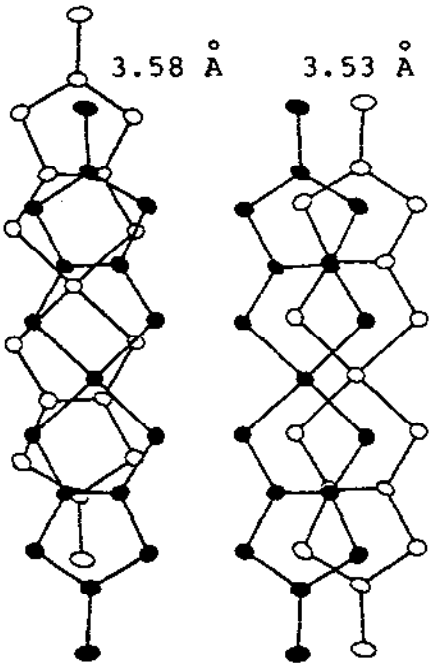

Fig. 7. Modes of molecular overlap in $(Me_4N)[Ni(dmit)_2]_2$.

observed at the transition temperature. No additional Bragg reflections could be seen in X-ray studies above 15 K, indicating that the resistivity anomaly around 100 K is not accompanied by a change in the periodicity of the lattice. Despite the sample dependence of the resistivity, every crystal shows a thermo-activated resistivity behaviour below ca. 10 K at ambient pressure.

The pressure-dependence of the resistivity has been reported up to 7 kbar (Fig. 8) [55]. Pressures above 3 kbar suppress the metal to semi-metal transition and a transition to a superconducting state is observed at low temperatures. The transition temperature, T_c, is 5 K at 7 kbar and the positive pressure effect ($dT_c/dp > 0$) is the same as in the case of $TTF[Ni(dmit)_2]_2$ [30,32] and the reverse of that of the organic donor superconductors.

(2) $(Et_4N)[Ni(dmit)_2]_2$. This material was synthesized using a method similar to that used for the $(Me_4N)[Ni(dmit)_2]_2$ salts.

The crystal structure of the black, elongated plates contains segregated stacks along *b* [63]. The columns consist of anion dimers with two independent S ··· S contacts of 3.691 and 3.610 Å, slightly shorter than the van der Waals distance. There are no short interdimer contacts within the stack. Many short S ··· S contacts are observed between the stacks while the side-by-side arrangement of $[Ni(dmit)_2]$ anions along the *c* axis is similar to that observed in some BEDT-TTF salts. The shortest

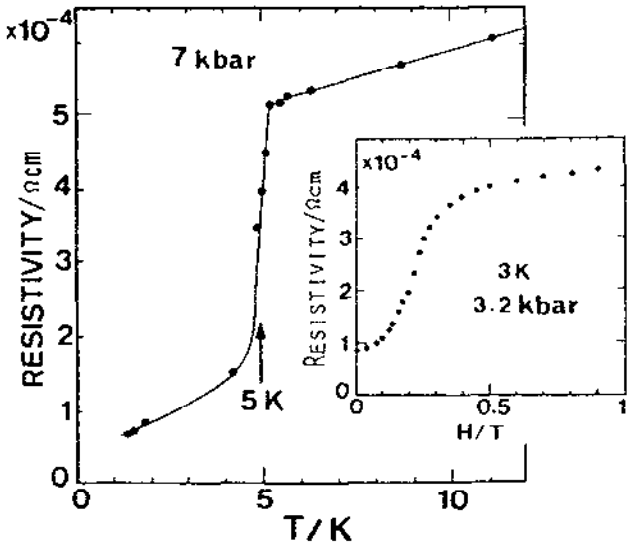

Fig. 8. Superconducting transition of $(Me_4N)[Ni(dmit)_2]_2$ at 7 kbar and 3 kbar (insert).

contacts are found between the sulphur atoms in the dithiolene (inner part) of the anion. Weak S ··· S interactions (3.903 Å) are found between the thioketone sulphur atoms. The Et_4N cations are located at the centre of the *ab* plane and are highly disordered. $(Et_4N)[Ni(dmit)_2]_2$ behaves like a semiconductor with a small anisotropy. The maximum value of the conductivity, 4.5×10^{-2} S cm^{-1}, was measured along the *b* axis [63].

(3) [Ni(dmit)$_2$] salts of mixed alkyl ammonium cations. Following the discovery of the low-temperature superconductor $(Me_4N)[Ni(dmit)_2]_2$, a series of $[Ni(dmit)_2]$ salts with cations (C) related to Me_4N^+ was investigated [54]. The salts include C = $Et_2Me_2N^+$, $EtMe_3N^+$, Me_4P^+, Me_4As^+, ... [67,68]. In all cases the $(C)[Ni(dmit)_2]_2$ salts were obtained by electrochemical oxidation. The most interesting of these salts is the $(Et_2Me_2N)[Ni(dmit)_2]_2$ which shows two distinct crystal forms, α and β. More recently, preliminary results on the $(H_yMe_{4-y}N)[Ni(dmit)_2]_2$ series of compounds have been reported [69–73].

The β-$(Et_2Me_2N)[Ni(dmit)_2]_2$ salt [68] has a crystal structure similar to that of the tetraalkylammonium salts discussed previously. The $Ni(dmit)_2$ anions are "dimerized" with weak inter-dimer interactions, explaining the semiconducting behaviour observed for this salt which has a room temperature conductivity of about 3 S cm^{-1}.

Crystals of the α-$(Et_2Me_2N)[Ni(dmit)_2]_2$ salt were grown from the same solution as the β form, but were obtained as hexagonal plates, as opposed to more elongated plates of the β form. The crystal structure of the α form is completely

different from that of the β form and contains a totally new mode of stacking for the $[Ni(dmit)_2]$ units [67]. Along the b axis, the $[Ni(dmit)_2]$ anions are arranged in a side-by-side fashion with short S ··· S distances (3.42–3.61 Å). In the c direction, the $[Ni(dmit)_2]$ anions show two types of overlap, one of which is a new type given the name "spanning overlap" (Fig. 9). Simple tight binding band calculations [67] indicate a 2-D Fermi surface very similar to that of the superconductors with κ-type molecular arrangement, viz. κ-(BEDT-TTF)$_2$I$_3$ and κ-(BEDT-TTF)$_2$Cu(NCS)$_2$, and are consistent with the results of the analysis of the optical reflectance spectra [57]. Metal-like conductivity was observed from room temperature (20–100 S cm^{-1}), down to 1.5 K, with no metal-to-semiconductor transition. However, preliminary pressure studies did not reveal a superconducting transition above 1.5 K at pressure up to 5 kbar [68].

Electrochemical oxidation of a mixture of $(C)[Ni(dmit)_2]/(C)ClO_4$ ($C = EtMe_3N^+$, Me_4P^+, Me_4As^+, Me_4Sb^+, $Me_3S(O)^+$, Me_3S^+) in acetonitrile-acetone (1:1) produces black plates of the corresponding $(C)[Ni(dmit)_2]_2$ fractional oxidation state salts [68]. The crystal structure for $C = EtMe_3N^+$, Me_4P^+, $Me_3S(O)^+$ has been determined by X-ray diffraction. $(EtMe_3N)[Ni(dmit)_2]_2$ is isostructural to the β-$(Et_2Me_2N)[Ni(dmit)_2]_2$ phase discussed above. The $Ni(dmit)_2$ anions are "dimerized" with weak inter-dimer interactions and this explains the semi-conducting behaviour observed in both salts which have room-temperature conductivity of $\approx$0.4 and 3 S cm^{-1}, respectively. In both salts, the counter cations are in a disordered state. The $(Me_4P)[Ni(dmit)_2]_2$ and $(Me_4As)[Ni(dmit)_2]_2$ salts are isostructural and do not have a conventional one-dimensional columnar structure [68]. Two $Ni(dmit)_2$ molecules form a pair with interplanar spacing of 3.32–3.33 Å; each pair is surrounded by six pairs to form a two-dimensional acceptor sheet. The room-temperature conductivities are 0.6 and 0.1 S cm^{-1}, respectively.

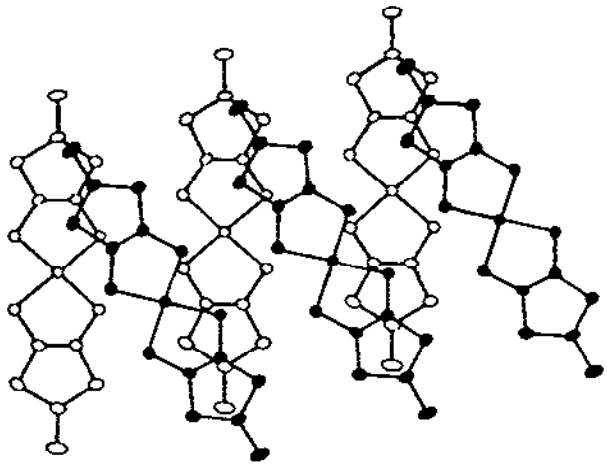

Fig. 9. "Spanning overlap" in α-$(Et_2Me_2N)[Ni(dmit)_2]_2$.

The crystal structure of the $(HMe_3N)[Ni(dmit)_2]_2$ compound is characterized by a "dimerization" within the stacks of $[Ni(dmit)_2]$ with alternating interplanar distances of 3.51 and 3.60 Å [69]. The temperature-dependent conductivity is quite unusual (Fig. 10): the crystal exhibits a metal-like behaviour from room temperature down to ≈120 K, at which temperature it undergoes a metal-to-insulator transition and then remains semiconducting down to ≈15 K. At this temperature it undergoes an insulator-to-metal transition and remains metallic down to 2 K [70,71]. A negative magnetoresistance appears below 20 K and decreases with decreasing temperature down to 3.8 K. At lower temperatures the magnetoresistance increases again and even becomes slightly positive below 2.5 K [71].

(4) Other fractional oxidation state $[Ni(dmit)_2]$ salts. A number of other salts of $[Ni(dmit)_2]$ have been reported in which the anion has a non-rational fractional charge [20,27,72–74,77–79]. A variety of methods, oxidation with bromine, electrocrystallisation or aerial oxidation of an acetone–water solution has been used to prepare these salts. The resulting salts have been shown to have conductivities increased by up to ten orders of magnitude compared with the starting material. However, very few of these compounds have been fully characterized as single crystals or their structures determined.

$(n\text{-}Bu_4N)_2[Ni(dmit)_2]_7 \cdot 2(CH_3CN)$ was prepared by galvanostatic oxidation

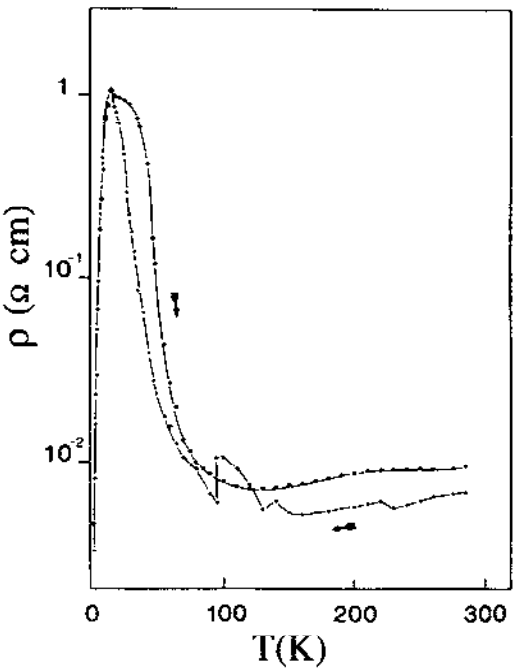

Fig. 10. Electrical resistivity of $(HMe_3N)[Ni(dmit)_2]_2$.

from an acetonitrile solution of the $(n\text{-}Bu_4N)[Ni(dmit)_2]$ salt and $(n\text{-}Bu_4N)ClO_4$ as supporting electrolyte [79]. Both needle and plate-like crystals were observed on the electrode. Whilst the structure of the plate-shaped crystals has been studied by X-ray, and is discussed below, the needle-shaped crystals were unsuitable for a full crystal structure determination, but X-ray powder patterns show the two types of crystals to be dissimilar.

The crystal structure of the plate-shaped crystals of $(n\text{-}Bu_4N)_2[Ni(dmit)_2]_7 \cdot 2(CH_3CN)$ is more complex than those of the previously studied tetraalkylammonium salts [20]. It can best be described as layers of $[Ni(dmit)_2]$ anions parallel to (001) separated by sheets of $(n\text{-}Bu_4N)^+$ cations and acetonitrile molecules. The layers contain stacks of acceptor anions along the [110] direction. These anions are further ordered into alternating centrosymmetric triads and tetrads. These triads and tetrads are tilted by 21° with respect to the stacking axis [110] (Fig. 11). Whilst there are a number of both inter- and intrastack short S ··· S contacts, the irregularity of stacking could well account for the fact that the material behaves like a semi-conductor with a room temperature conductivity of 1–10 S cm^{-1}. The degree of anisotropy in the conductivity along the different directions of the crystal is reported as low. A plot of log σ vs. $1/T$ is non-linear throughout the temperature range 300–30 K, which might be explained by either the material undergoing subtle structural changes or by changes in the carrier concentration [20].

The $(Ph_4As)[Ni(dmit)_2]_4$ compound was studied to see whether the more rigid nature of the cation would prevent the configurational disorder often found in the

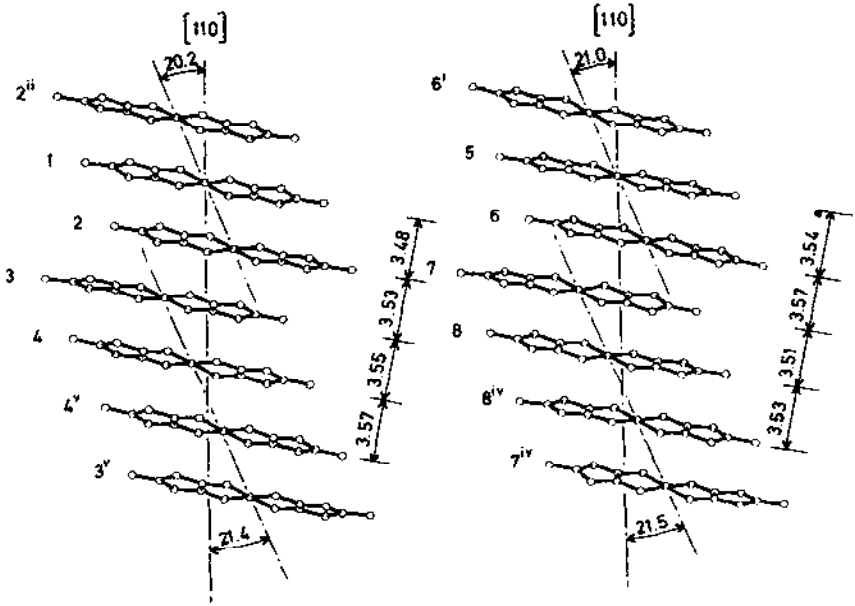

Fig. 11. Stacking mode in $(n\text{-}Bu_4N)_2[Ni(dmit)_2]_7 \cdot 2CH_3CN$.

R_4N^+ salts [74]. Slow interdiffusion of $(Ph_4As)[Ni(dmit)_2]$ and I_2/NaI solution in CH_3CN yielded both black, shiny needles and platelets. The structure of the needle-shaped crystals consists of stacks of $[Ni(dmit)_2]$ tetrads. The interplanar stacking distances are 3.53 and 3.50 Å and there are a number of close interstack distances. The room-temperature conductivity along the long axis of the needle-shaped crystals and along the longest direction of the (001) face of the platelets was 10–15 S cm^{-1}. The compound behaves like a semiconductor with a non-linear relationship of log σ to $1/T$. Above 26 K, the conductivity is almost temperature-independent. The anisotropy $\sigma_a:\sigma_b:\sigma_c$ was $1:1:10^{-5}$ compared with $2:1:10^{-4}$ for $(n\text{-}Bu_4N)_2[Ni(dmit)_2]_7 \cdot 2(CH_3CN)$ and 1:50:8 for $(Et_4N)[Ni(dmit)_2]_2$.

$(H_4N)_x[Ni(dmit)_2]$ phases have been also reported, but were not fully characterized [72,73]. Investigations on the "long-chain" $[Me_2(C_nH_{2n+1})_2Ni(dmit)_2]$ salts should also be mentioned for they open a new research area in the preparation of conductive Langmuir–Blodgett films [75,76].

(iv) [Ni(dmit)$_2$] salts with inorganic cations

Initial reports indicated that compounds with $M_x[Ni(dmit)_2]$ stoichiometry (where M is Li or Na, $0<x<0.5$) were semiconducting [77,80]. Recent and more detailed work shows that well-defined salts, $M[Ni(dmit)_2]_2$ (M = Li, Na, or K), can be obtained by electrocrystallization of acetonitrile solutions of $(n\text{-}Bu_4N)_2[Ni(dmit)_2]$ in the presence of a large excess of Group 1 metal cations [81,82]. These are listed in Table 3.

(a) Li[Ni(dmit)$_2$]$_2 \cdot 2CH_3CN$

Electrochemical synthesis generated poorly formed plate-like crystals with $Li[Ni(dmit)_2]_2 \cdot 2CH_3CN$ stoichiometry. Variable temperature conductivity studies on a compressed pellet showed the material to be a well-behaved semiconductor

TABLE 3

$[Ni(dmit)_2]$ salts with inorganic cations

Compound	σ_{RT}/S cm^{-1} [a]	Crystal structure ref.	Other ref.
$Li[Ni(dmit)_2]_2 \cdot 2CH_3CN$	≈0.5 (sc)		81
$Na[Ni(dmit)_2]_2$	≈20 (m)		72,73,81
$K_{0.4}[Ni(dmit)_2]$	≈100 (m)		82
$Rb_{0.36}[Ni(dmit)_2]$	≈10 (sc)		81
$Cs[Ni(dmit)_2]_2$			81

[a] m = metal-like conductivity; sc = semiconductor-like conductivity.

(300–40 K) with an activation energy of ~0.02 eV and a room-temperature conductivity of ~0.6 S cm^{-1} [81].

(b) Na[Ni(dmit)$_2$]$_2$

Electrocrystallization produced well-formed needles of Na[Ni(dmit)$_2$]$_2$. Electrical conduction studies showed a metallic behaviour with a room-temperature conductivity of ~100 S cm^{-1}. This metallic state is maintained with decreasing temperature and the crystals behave as a simple metal down to 2 mK at atmospheric pressure but without sign of a superconducting transition. Under pressures of 3 and 5.7 kbar, the crystals show the expected decrease in resistivity and retention of the metallic state to lower temperatures but no sign of a superconducting transition (Fig. 12) [81].

Thermopower measurements show negative values over the entire temperature range (300–2 K), indicating electrons to be the principal carriers. To date, poor crystal quality has prevented a full structure determination, although initial X-ray oscillation photographs indicate the system to be essentially one-dimensional with a regular spacing of 3.79 Å [83].

(c) K$_{0.4}$[Ni(dmit)$_2$]

Analyses of the poorly formed plates of this compound indicate a K$_{0.4}$[Ni(dmit)$_2$] stoichiometry. The room-temperature conductivity along the longest axis of

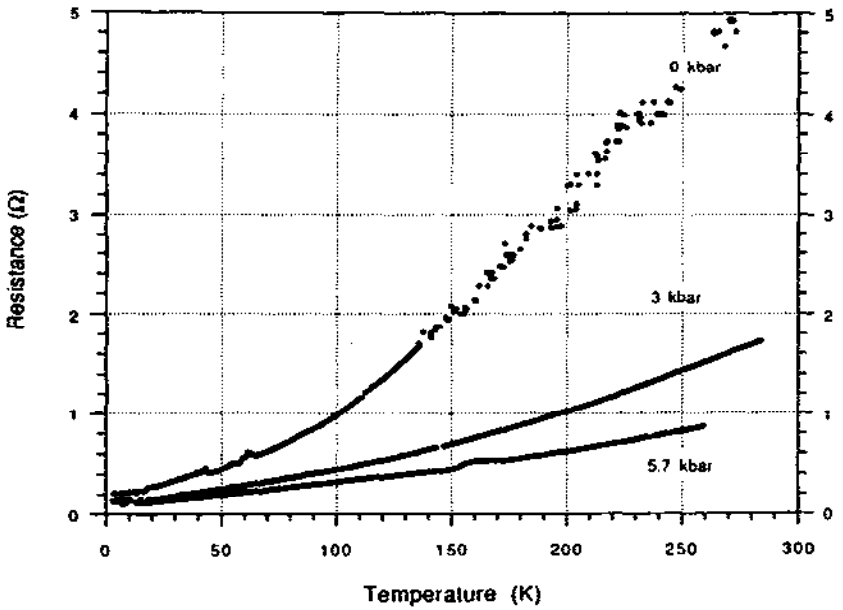

Fig. 12. Temperature dependence of the resistance of Na[Ni(dmit)$_2$]$_2$ at 1 bar, 3 and 5.7 kbar.

the plate was found to lie between 10 and 230 S cm^{-1}. The temperature dependence of the conductivity was studied for numerous crystals, the majority of which did not show a clear transition from metallic to semiconductor state. Some crystals showed a steady increase in conductivity down to 20 K, whilst others exhibited a fall in conductivity after an initial rise. Poor crystal quality has prevented the identification of any precise transition temperature and has also prevented a full crystal structure determination [82]. Initial X-ray oscillation photographs, however, show the compound to possess a regular stacked structure with a mean interplanar distance of ≈ 3.72 Å [73,83]. Pressure studies show that transition temperatures are raised with increasing pressure whilst the activation energy is unchanged [84].

(d) $M_x[Ni(dmit)_2]$ ($M = Rb$ or Cs)

Only small quantities of fibrous materials have been obtained which give $Rb_{0.36}[Ni(dmit)_2]$ and $Cs[Ni(dmit)_2]_2$ stoichiometries. The extremely poor quality of the crystals grown has prevented any detailed study [73,81].

D. $[Pd(dmit)_2]$ COMPOUNDS

The unusual properties of the salts of $[Ni(dmit)_2]$ have stimulated the study of the preparation of the palladium analogues. Discussion of the palladium compounds will be divided into sections, similar to those used for the nickel compounds.

(i) $[Pd(dmit)_2]$ salts with "open-shell" organic cations

The salts reported [22,27,37,42,43,47,48,80,85–91], together with some of their physical properties, are listed in Table 4. A less extensive range of compounds than for nickel has been reported and all exhibit semiconducting behaviour at room temperature except for the TTF salt.

The $TTF[Pd(dmit)_2]_2$ compound was prepared in a manner similar to that of the nickel analogue [22], i.e. by slow interdiffusion of saturated solutions of $(TTF)_3(BF_4)_2$ and $(n\text{-}Bu_4N)[Pd(dmit)_2]$. This preparation yields mainly black shiny needles (α phase). In some experiments, crystals of another needle-shaped phase (α' phase) have been isolated. Moreover, a few plate-shaped crystals (δ phase) could also be sorted out from the predominantly needle-like crystals [87]. As evidenced by X-ray diffraction crystal structure determination, the three species have the same $TTF[Pd(dmit)_2]_2$ stoichiometry [87]. The occurrence of several phases for this compound complicates its study.

(a) α-$TTF[Pd(dmit)_2]_2$

This phase is isostructural (monoclinic, C-centred) with $TTF[Ni(dmit)_2]_2$ (Fig. 13) [22,87]. Shorter interplanar distances are observed within the $[M(dmit)_2]$

TABLE 4

[Pd(dmit)$_2$] salts with "open-shell" organic cations

Compound	σ_{RT}/S cm^{-1} [a]	Crystal structure ref.	Other ref.
α-TTF[Pd(dmit)$_2$]$_2$	750 (m–sc ≈ 220 K)[b]	22	80,85–87
α′-TTF[Pd(dmit)$_2$]$_2$	750 (m–sc ≈ 200 K)[b]	87	43,47,48,88–90
δ-TTF[Pd(dmit)$_2$]$_2$	100 (m–sc ≈ 120 K)[b]	87	43,91
(depz)$_{0.3-0.35}$[Pd(dmit)$_2$]	≈10^{-3}		42
(bpy)$_2$[Pd(dmit)$_2$]$_5$	≈0.76 (sc)		27
(bpy)$_{0.7}$[Pd(dmit)$_2$]	≈1.6×10^{-2} (sc)		27
TMTTF[Pd(dmit)$_2$]$_y$	≈1.5×10^{-3}		37
TMTSF[Pd(dmit)$_2$]	≈2		37
TSeF[Pd(dmit)$_2$]	(sc)		80
TTT$_{1.2}$[Pd(dmit)$_2$]	≈100 (sc)		80
TSeT$_{1.2}$[Pd(dmit)$_2$]	≈100 (sc)		80
(perylene)$_2$[Pd(dmit)$_2$]	≈100 (sc)		80

[a] m = metal-like conductivity; sc = semiconductor-like conductivity.
[b] Measurement on single crystal, remainder measured on compressed pellet.

and TTF stacks, in the α phase of the palladium compound (3.44 and 3.54 Å, respectively) compared with 3.55 and 3.65 Å in the nickel compound.

The room-temperature conductivity measured along [010] (750 S cm^{-1}) is significantly higher than that of the nickel compound. On cooling, the crystals exhibit

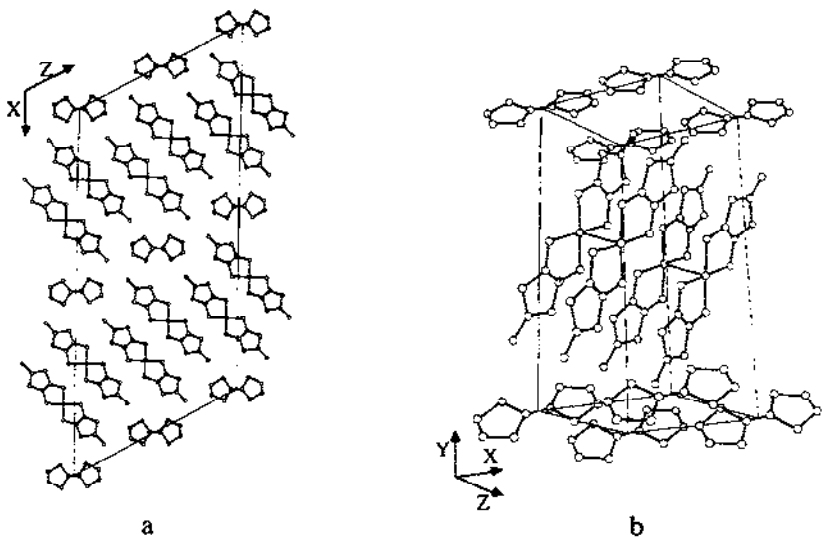

Fig. 13. Crystal structure of (a) α- and α′-TTF[Pd(dmit)$_2$]$_2$, and (b) of δ-TTF[Pd(dmit)$_2$]$_2$.

increasing conductivities down to 220 K, below which temperature the crystals behave like semiconductors with a low activation energy ($\Delta E = 0.01$ eV).

X-ray studies have revealed that a phase change occurs at about 220 K, leading to a lower symmetry triclinic β phase [87]. When these crystals are warmed back to room temperature, a phase change occurs again at 230–240 K, yielding, after several cycles of temperature, a triclinic high-temperature modification (γ phase). However, the crystals then behave as semiconductors when cooled. The $\alpha \rightarrow \beta \rightarrow \gamma$ transition is then irreversible. The effect of pressure is the suppression of the irreversible metal-to-semiconductor transition described above, while a superconducting transition occurs at 1.7 K and 22 kbar [89].

(b) α′-TTF[Pd(dmit)$_2$]$_2$

Some needle-shaped crystals, also isostructural (monoclinic, C-centred) with TTF[Ni(dmit)$_2$]$_2$, and apparently bearing no differences with the α phase crystals described above, were observed to retain their initial monoclinic symmetry down to 100 K. This phase, called α', exhibits the same room-temperature conductivity (750 S cm^{-1}) and also undergoes a metal-to-insulator transition at ≈ 200 K. However, this transition is completely reversible and shows no hysteresis [87].

The effect of high pressure (>16 kbar) is again the suppression of this metal-to-insulator transition [88] while a complete superconducting transition is observed at rather higher temperatures, for example 5.93 K at 24 kbar [89]. Analysis of the temperature–pressure phase diagram of the α' phase reveals the absence of 1-D instabilities such as spin Peierls and spin density wave ground states. On the other hand, a gradual localization of the carriers is observed at low pressures [88,89] which can be related to a charge density wave condensation evidenced by X-ray diffuse scattering experiments [48,49]. Therefore, α'-TTF[Pd(dmit)$_2$]$_2$ is the first example in which competition between CDW and superconductivity is observed. These results, and their comparison with those obtained for the nickel analogue compound, TTF[Ni(dmit)$_2$]$_2$, have been correlated with the band structure of these unusual multi-Fermi surface systems [43]. Related ESR studies have also been reported [88].

(c) δ-TTF[Pd(dmit)$_2$]$_2$

The δ phase refers to the plate-shaped crystals obtained together with the needle-shaped α and α' crystals. In this phase, the [Pd(dmit)$_2$] species form dimers with a Pd–Pd bond distance as short as 3.11 Å (the next inter-dimer shortest Pd ··· Pd distance is 5.31 Å) [87]. These dimers are also characterized by a folding of the [Pd(dmit)$_2$] units; the dihedral angle between two dmit moities of the [Pd(dmit)$_2$] units is 6.3°. The room-temperature conductivity measured along the a direction is 100 S cm^{-1}. Surprisingly for such a dimerized system, this compound displays metallic character down to 120 K, at which temperature it undergoes a reversible metal-to-insulator transition. However, although this compound does not possess a stack structure, the structural 2-D character is evidenced by short intra- and interstack

S ··· S interactions, resulting in a low anisotropy in the conductivities in the (010) platelet plane: $\sigma_a:\sigma_b:\sigma_c = 100:20:(5\times10^{-2})$ [87]. In this strongly dimerized system, tight-binding band calculation shows that only the HOMO band is partially filled and that the metal-to-insulator transition at 120 K could be due to nesting of the Fermi surface [43].

(d) TMTSF[Pd(dmit)$_2$]$_2$ and TMTTF[Pd(dmit)$_2$]$_2$

Both these compounds were prepared by electrocrystallization. In the case of TMTSF[Pd(dmit)$_2$], the crystals were too small for extensive X-ray and conductivity studies, but the powder conductivity is promisingly quite high, 2 S cm^{-1}, i.e. ten times higher than that of the nickel analogue [37]. The powder conductivity of TMTTF[Pd(dmit)$_2$] is much lower, 5×10^{-4} S cm^{-1} [37].

(e) Miscellaneous

The TTT$_{1.2}$[Pd(dmit)$_2$], TSeT$_{1.2}$[Pd(dmit)$_2$] and (perylene)$_2$[Pd(dmit)$_2$] compounds have been mentioned [80] as exhibiting extremely high powder conductivities (>100 S cm^{-1}) but no detailed single-crystal studies have confirmed these preliminary results.

(ii) [Pd(dmit)$_2$] salts with "closed-shell" organic cations

These salts have been less studied [27,53,55,60–62,86,91–96] than their nickel counterparts and those that have been studied are shown in Table 5.

TABLE 5

[Pd(dmit)$_2$] salts with "closed-shell" organic cations

Compound	σ_{RT}/S cm^{-1} [a]	Crystal structure ref.	Other ref.
(n-Bu$_4$N)$_{0.5}$[Pd(dmit)$_2$]	12 (m–sc 240 K)[b]	91	86
(n-Bu$_4$N)$_{0.33}$[Pd(dmit)$_2$]	150 (m–sc 120 K)[b]	91	
(n-Bu$_4$N)$_{0.28}$[Pd(dmit)$_2$]	≈1		27
(Et$_4$N)$_{0.44}$[Pd(dmit)$_2$]	≈1		27
(Et$_4$N)$_{0.5}$[Pd(dmit)$_2$]	1.1×10^{-1} (sc)[b]	53	60–62,92
(Me$_4$N)$_{0.52}$[Pd(dmit)$_2$]	≈1		27
α-(Me$_4$N)$_{0.5}$[Pd(dmit)$_2$]	50 (sc)[b]	55	96
β-(Me$_4$N)$_{0.5}$[Pd(dmit)$_2$]	50 (sc)[b]	55	96
(Me$_4$N)$_x$[Pd(dmit)$_2$]	28 (sc)[b]		93
(Me$_4$As)$_{0.5}$[Pd(dmit)$_2$]	1 (sc)[b]	96	

[a] m = metal-like conductivity; sc = semiconductor-like conductivity.

[b] Measurement on single crystal, remainder measured on compressed pellet.

(a) Dianion and mono-anion salts

Except for their preparation [53,94], very few studies on these salts have been reported. In an interesting paper dedicated to EPR studies on single crystals of $(n\text{-}Bu_4N)[M/M'(dmit)_2]$ (M = Ni, Pd, Pt; M' = Au) [94], Kirmse et al. concluded, on the basis of molecular orbital calculations, that the half-filled molecular orbital has a b_{2g} symmetry resulting from a linear combination of the metal d_{xz} orbital and the out-of-plane $3p_x$ orbitals of the four sulphur atoms. The unpaired electron associated with the $[M(dmit)_2]^-$ anion is centred on the ligand system and principally on the sulphur atoms. This result has been confirmed by electrochemistry–ESR coupled studies on the M(dmit)(dppe) series of compounds (M = Ni, Pd, Pt; dppe = 1,2-bis-diphenylphosphinoethane) [95].

(b) Fractional oxidation state salts

(1) $(n\text{-}Bu_4N)_x[Pd(dmit)_2]$. The most extensively studied fractional oxidation salts are the $(n\text{-}Bu_4N)^+$ salts. It has been reported that electrochemically grown crystals possess a $(n\text{-}Bu_4N)_x[Pd(dmit)_2]$ range of stoichiometries $(0.2 < x < 0.7)$ [91].

Electrochemical growth of crystals from an acetonitrile solution of $(n\text{-}Bu_4N)[Pd(dmit)_2]$ and $(n\text{-}Bu_4N)ClO_4$ at constant current (1 μA) gave, amongst other products, plate-like crystals of $(n\text{-}Bu_4N)_{0.5}[Pd(dmit)_2]$ and twisted needle-like crystals of $(n\text{-}Bu_4N)_{0.33}[Pd(dmit)_2]$ [91].

The full crystal structure could not be determined on either compound since the $(n\text{-}Bu_4N)$ cations are highly disordered and show only regions of residual electron density. In both cases, the structure consists of $[Pd(dmit)_2]_2$ dimers stacked along [100] forming layers in the (010) plane. The intra-dimer Pd–Pd bond distance is 3.039 and 3.048 Å in $(n\text{-}Bu_4N)_{0.5}[Pd(dmit)_2]$ and $(n\text{-}Bu_4N)_{0.33}[Pd(dmit)_2]$, respectively, resulting in an unusual eclipsed overlap of the two $[Pd(dmit)_2]$ entities and folding of the normally planar complexes [91]. There are various short S ··· S interactions, giving both compounds a two-dimensional character. The structure is similar to that found for δ-$TTF[Pd(dmit)_2]_2$ where sheets of $[Pd(dmit)_2]_2$ dimers alternate with sheets of TTF cations [87,91].

The room-temperature conductivity of $(n\text{-}Bu_4N)_{0.5}[Pd(dmit)_2]$, measured along [100] is $\approx 12\ S\ cm^{-1}$. On cooling, this phase exhibits a metallic conductivity down to 240 K. At this point, a gradual change to a semiconducting state is observed, which proved to be reversible on warming, with the metallic state regained. This system is similar to the δ-$TTF[Pd(dmit)_2]_2$ system.

The room-temperature conductivity of $(n\text{-}Bu_4N)_{0.33}[Pd(dmit)_2]$ measured along the needle [100] axis is somewhat higher, viz. $150\ S\ cm^{-1}$. Studies of the temperature-dependence of the conductivity shows metallic behaviour down to 120 K, at which point a metal-to-insulator transition occurs. This transition was proved to be irreversible on warming, with the crystal behaving as a semiconductor

over the entire range. This behaviour is similar to that observed for α-TTF[Pd(dmit)$_2$]$_2$.

(2) (Me$_4$N)[Pd(dmit)$_2$]$_2$. There are two polymorphs of (Me$_4$N)[Pd(dmit)$_2$]$_2$, a triclinic form (α) and a monoclinic form (β) [55,96].

The black plate-type crystals of the α form were obtained by electrochemical oxidation from a solution of (Me$_4$N)Pd(dmit)$_2$] and (Me$_4$N)ClO$_4$ in acetonitrile for six weeks using a 0.6 μA constant current. The crystal structure is similar to that of (Me$_4$N)[Ni(dmit)$_2$]$_2$. There are two crystallographically independent Pd(dmit)$_2$ molecules, which form columns along the two directions [010] and [011]. In these columns, two Pd(dmit)$_2$ molecules form a weak M ··· M dimer with Pd ··· Pd distances of 3.17 and 3.13 Å. X-ray photographs of the α form taken at 103 K show an $a \times 2b \times 2c$ structure.

The room-temperature conductivity of this phase is 50 S cm^{-1}. The resistivity is almost constant at room temperature, slightly increases with decreasing temperature, and begins to increase rapidly at ≈100 K. The pressure dependence of the resistivity of the α form was measured up to 12 kbar. A clearly metallic behaviour was observed above 6 kbar [96].

The β form was obtained by leaving the solution of (Me$_4$N)[Pd(dmit)$_2$] and (Me$_4$N)ClO$_4$ in acetonitrile for four months. Although the Pd(dmit)$_2$ molecules form dimeric structures, the crystal structure of the β form is similar to that of (Me$_4$N)-[Ni(dmit)$_2$]$_2$ except for the cation sites. The Pd(dmit)$_2$ molecules form 1D stacks along the [110] and [1$\bar{1}$0] directions forming dimeric structures. The room-temperature conductivity of the β form is ≈50 S cm^{-1} and its conducting behaviour is similar to that of the α form [55,96].

(Me$_4$N)$_x$[Pd(dmit)$_2$] has been reported as needle-shaped crystals by air oxidation of (Me$_4$N)[Pd(dmit)$_2$]. At atmospheric pressure, the compound exhibited a room-temperature conductivity of 28 S cm^{-1} and a metal-to-insulator transition around room temperature. At 5 kbar, the transition is lowered to 20 K [93].

(3) (Me$_4$As)[Pd(dmit)$_2$]$_2$. The crystal structure [96] is similar to that of β-(Me$_4$N)[Pd(dmit)$_2$]$_2$ except for the cation sites. The Pd(dmit)$_2$ molecules form 1D stacks along the [110] and [1$\bar{1}$0] directions, containing dimers similar to those observed in β-(Me$_4$N)[Pd(dmit)$_2$]$_2$.

This salt shows semiconducting behaviour and its room-temperature conductivity is ≈1 S cm^{-1} with an activation energy of 0.07 eV.

(4) (Et$_4$N)$_{0.5}$[Pd(dmit)$_2$]. Studies on the structure and electrical behaviour of (Et$_4$N)$_{0.5}$[Pd(dmit)$_2$] have been also reported [53,60–62,92].

(iii) [Pd(dmit)$_2$] salts with inorganic cations

As with the nickel and platinum complexes, the salts of [Pd(dmit)$_2$] with Group 1 cations have been studied. The compounds studied [49,57,81,97–99] are listed in Table 6.

(a) Cs[Pd(dmit)$_2$]$_2$

This salt was obtained [98] as well-formed black plates deposited on the anode by electrocrystallization over a period of seven days of an acetonitrile solution containing (n-Bu$_4$N)[Pd(dmit)$_2$] and $CsPF_6$ using Pt wire electrodes and a current density of $\approx 6\ \mu A\ cm^{-2}$.

(1) Crystal structure. The crystal structure of Cs[Pd(dmit)$_2$]$_2$ as viewed along the b axis is shown in Fig. 14 [97]. The [Pd(dmit)$_2$] anions are stacked along [110] forming an apparent four-fold structure. However, because of the C-centred lattice, the real repeat unit contains two anions. The intra-dimer separation is 3.299 Å and the

TABLE 6

[Pd(dmit)$_2$] salts with inorganic cations

Compound	σ_{RT}/S cm^{-1} [a]	Crystal structure ref.	Other ref.
Na[Pd(dmit)$_2$]$_2$			81
K[Pd(dmit)$_2$]$_2$	≈ 45 (sc)		81
Rb$_2$[Pd(dmit)$_2$]$_4$·CH$_3$CN	≈ 1 (sc)		81
Cs[Pd(dmit)$_2$]$_2$	≈ 200 (m–sc ≈ 60 K)[b]	97	49,57,98

[a] m = metal-like conductivity; sc = semiconductor-like conductivity.
[b] Measurement on single crystal, remainder measured on compressed pellet.

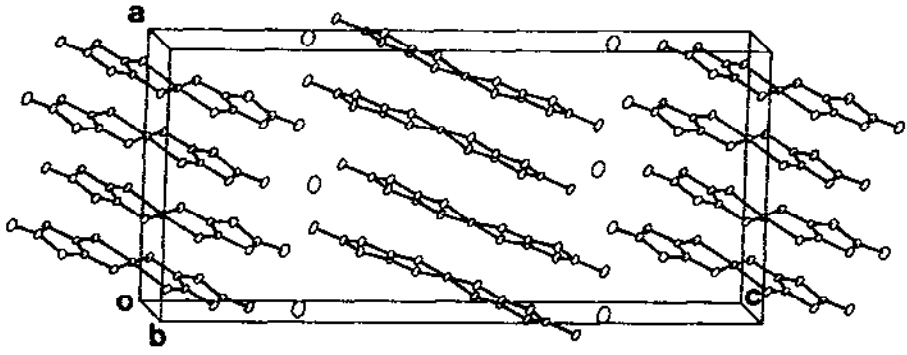

Fig. 14. Crystal structure of Cs[Pd(dmit)$_2$]$_2$.

interdimer separation is 3.762 Å. The mode of overlap of the dimers is shown in Fig. 15. It can be seen that, within the dimers, the two anions adopt an eclipsed configuration but between dimers the anions are slipped. However, the slipped configuration is one which still appears to retain a large number of S ··· S interactions. The Cs^+ cations occupy channels in the *b* direction. Each Cs^+ is surrounded by six S atoms at 3.589, 3.636 and 3.796 Å.

(2) Electrical conductivity and thermopower. The electrical conductivity of this compound has been reported to be approximately 200 S cm^{-1} at room temperature [98]. The temperature-dependence of the conductivity is that of a metal down to ≈ 60 K where there is a transition to a semiconducting behaviour. Under pressures of 3 and 6 kbar, the transition temperature is reduced to 50 and 25 K, respectively, and the transition disappears for some samples at 9 kbar [99]. No evidence of superconductivity was observed at pressures up to 20 kbar and temperatures down to 1.4 K.

A study of the thermopower of the compound shows the expected transition from metal to semiconductor at 56.5 K at ambient pressure. Within the metallic region, the sign of the thermopower is negative, indicating that the carriers are electrons [99].

(3) Magnetic susceptibility. The sample was found to be paramagnetic with a drop observed in χ just above 50 K. The Pauli susceptibility is within the range usually found for the metallic charge transfer salts of BEDT-TTF. Below 40 K, there is clearly a significant Curie tail from paramagnetic defects. When the influence of the

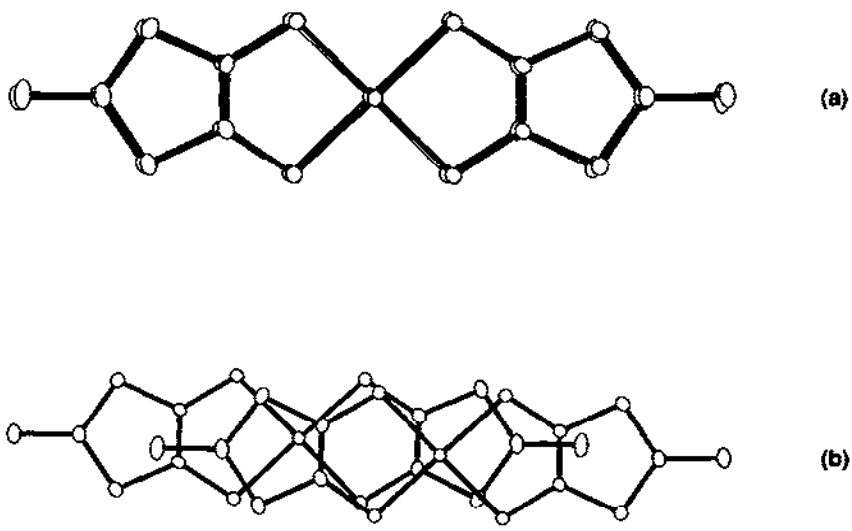

Fig. 15. Mode of overlap in $Cs[Pd(dmit)_2]_2$. (a) Within the "dimers"; (b) between "dimers".

Curie tail is subtracted from the data, the transition appears to be a simple Peierls transition [99].

(4) Optical studies. From polarized optical studies, it appears that the system is essentially two-dimensional within the metallic region. From the reflectance spectra, the two-dimensional dispersion at $10\,000\,cm^{-1}$ appears to be an intermolecular charge-transfer excitation within the $[Pd(dmit)_2]_2$ dimer [57].

(5) X-ray diffuse scattering. Evidence for a low-temperature structural distortion was obtained from X-ray scattering patterns, which showed two types of intense satellite reflection present below 56.5 K [43,99]:

(a) incommensurate superlattice spots, $q_i=(1,(1-\delta)/2,0)$ where $\delta\approx0.04$, with respect to the main Bragg reflections of the high temperature C-centred monoclinic lattice, and

(b) commensurate Bragg reflections at $q_B=(1,0,0)$ which break the C-centred monoclinic symmetry of the high temperature structure.

Pre-transitional fluctuations are seen only for the incommensurate satellite reflections and these can be detected up to 100 K. The incommensurate satellite reflection intensity extrapolates to zero at $T_p=56.5\pm1$ K.

(b) Other [Pd(dmit)$_2$] salts with inorganic cations

Electrocrystallization of a solution of $(n\text{-}Bu_4N)_2[Pd(dmit)_2]$ with a 30-fold excess of $NaClO_4$ gave poorly formed crystals of $Na[Pd(dmit)_2]_2$. A compressed disc of this material exhibited a room temperature conductivity of $\approx3\,S\,cm^{-1}$ and behaved as a semiconductor on cooling with an activation energy of 0.061 eV [81]. Black needles of $K[Pd(dmit)_2]_2$ were obtained under similar conditions using $KClO_4$ and exhibited a conductivity of $0.5\,S\,cm^{-1}$ at room temperature. Single crystals showed a rise in conductivity down to 275 K where a gradual transition was observed to a semiconductive state. $Rb_2[Pd(dmit)_2]_4\cdot CH_3CN$ was also obtained as black needles under similar conditions and exhibits a room temperature conductivity of $\approx5\,S\,cm^{-1}$ and semiconducting behaviour with an activation energy of 0.035 eV [81].

E. [Pt(dmit)$_2$] COMPOUNDS

The range of materials reported is not as extensive as for nickel compounds. In every case, regardless of the cation, all the platinum compounds behave like semiconductors, although a wide variety of crystal structures and stoichiometries is observed.

(i) [Pt(dmit)$_2$] complexes with "open shell" organic cations

The principal salts studied [22,42,100] are given in Table 7.

(a) TTF[Pt(dmit)$_2$]$_3$

The platinum salt has a stoichiometry, TTF[Pt(dmit)$_2$]$_3$, different from those of the nickel and palladium compounds, TTF[M(dmit)$_2$]$_2$, precluding any direct comparison.

The crystal structure of TTF[Pt(dmit)$_2$]$_3$ contains stacks of [Pt(dmit)$_2$] monomers and [Pt(dmit)$_2$]$_2$ dimers alternating along [110] (Fig. 16) [22]. Within the dimers, the anions are eclipsed with a Pt–Pt bond distance of 2.935 Å. There are alternating layers of [Pt(dmit)$_2$] and [Pt(dmit)$_2$]$_2$ entities and of TTF molecules, parallel to the (001) plane. A number of short S ··· S contacts are found within and between the [Pt(dmit)$_2$] stacks, thus forming a two-dimensional network in the (001) plane.

The room-temperature conductivity measured along the [110] needle axis is 20 S cm^{-1} and the crystals behave like semiconductors from 300 and 100 K with a low activation energy (=0.04 eV) between 300 and 200 K [22].

(b) (HMTTeF)$_2$[Pt(dmit)$_2$]

There is considerable interest in replacing the S atoms in TTF-type molecules by Te atoms since this should result in larger intra-chalcogenide interactions. Electrocrystallization of a solution containing HMTTeF and (n-Bu$_4$N)[Pt(dmit)$_2$] yielded black plates of (HMTTeF)$_2$[Pt(dmit)$_2$] [100]. It can be seen that the stoichiometry is quite different from the TTF salt.

The crystal structure consists of tetradic columns of HMTTeF as illustrated in Fig. 17. The tetradic columns link together via Te ··· Te contacts to form a 2D network. The [Pt(dmit)$_2$] anions are located in the space between the two-dimensional HMTTeF tetrads with their molecular planes almost perpendicular to the HMTTeF molecules. It is interesting to note that the structure of TTF[Pt(dmit)$_2$]$_3$

TABLE 7

[Pt(dmit)$_2$] salts with "open shell" organic cations

Compound	σ_{RT}/S cm^{-1} [a]	Crystal structure ref.	Other ref.
TTF[Pt(dmit)$_2$]$_3$	20 (sc)[b]	22	
(HMTTeF)$_2$[Pt(dmit)$_2$]	20 (sc)[b]	100	
(depz)$_{0.3}$[Pt(dmit)$_2$]	5×10^{-2} (sc)		42

[a]sc = semiconductor-like conductivity.

[b]Measurement on single crystal, remainder measured on compressed pellet.

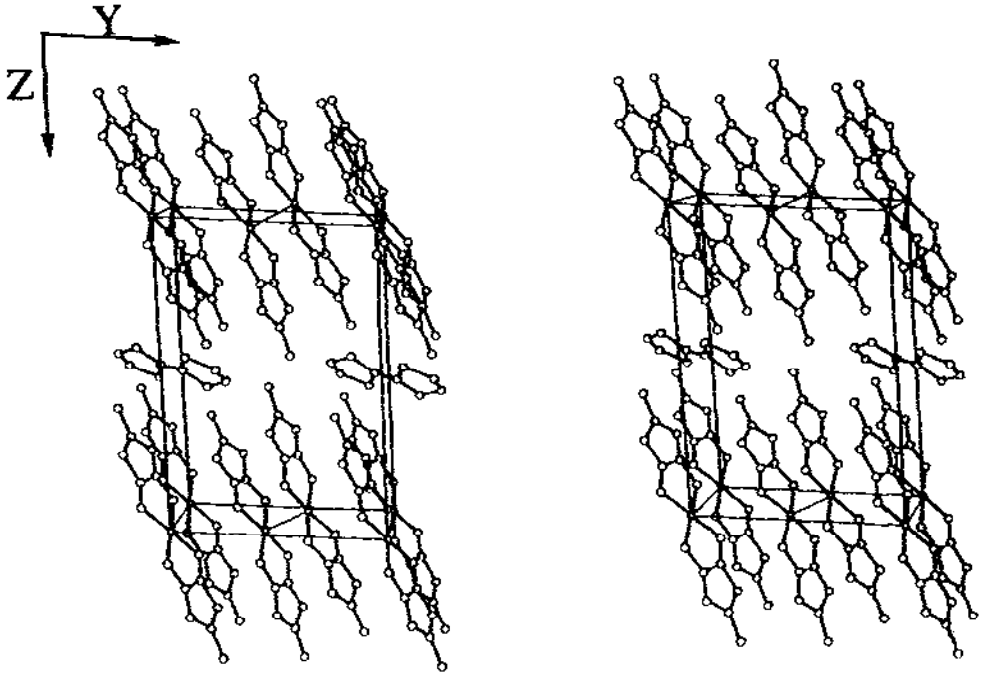

Fig. 16. Stereoscopic view of the unit cell of $TTF[Pt(dmit)_2]_3$.

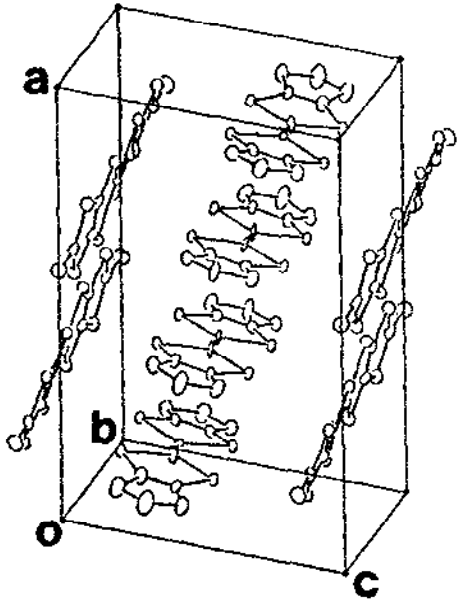

Fig. 17. Crystal structure of $(HMTTeF)_2[Pt(dmit)_2]$.

is dominated by [Pt(dmit)$_2$] columns and interactions, but that the replacement of TTF with HMTTeF produces a structure dominated by the organic cations and their interactions.

The conductivity of (HMTTeF)$_2$[Pt(dmit)$_2$] is 20 S cm^{-1} at room temperature and the compound exhibits semiconductor behaviour. Simple tight-binding band calculations suggest the absence of a Fermi surface in agreement with the conductivity results.

(ii) Other [Pt(dmit)$_2$] compounds

(a) (Me$_4$N)[Pt(dmit)$_2$]$_2$

This compound is isostructural with β-(Me$_4$N)[Pd(dmit)$_2$]$_2$. The electrical conductivity measurements have revealed a "metal–insulator transition" at 220 K, where a periodic lattice modulation begins to appear. The room-temperature conductivity is 10 S cm^{-1} [101].

(b) (n-Bu$_4$N)[Pt(dmit)$_2$]

In the structure of this compound, the [Pt(dmit)$_2$] anions are located in gaps formed by the (n-Bu$_4$N) cations and linked by short S $\cdots$ S intermolecular contacts into infinite zigzag bands along the c axis. The temperature-dependence of the magnetic susceptibility indicates antiferromagnetic interactions [102].

(c) (n-Bu$_4$N)$_x$[Pt(dmit)$_2$] with $0 < x < 0.5$

Although metallic behaviour was deduced from the reflectance spectra [78], the properties of this salt have not been fully characterized [25,77].

(d) Na[Pt(dmit)$_2$]$_2$

Electrical conductivity studies show this material to have a room temperature conductivity of $\approx 10^{-5}$ S cm^{-1}, and the crystal structure shows that the sodium ions are in a disordered state throughout the crystal lattice [81,103].

F. DMIT COMPOUNDS OF OTHER METALS

(i) [Fe(dmit)$_2$] compounds

The reaction of FeCl$_3$ with Na$_2$(dmit) gives the red soluble Na[Fe(dmit)$_2$] compound which, upon treatment with (n-Bu$_4$N)Cl, yields (n-Bu$_4$N)[Fe(dmit)$_2$] as green-brown crystals. The magnetic moment of 2.0 BM and Mössbauer data are consistent with a square coplanar complex. The salt was reported to be an insulator [104–106].

Oxidation of the (n-Bu$_4$N)[Fe(dmit)$_2$] salt by I$_2$ led to the formation of insoluble compounds sometimes containing intercalated solvent and I$_2$ with formulae such as

$(n\text{-}Bu_4N)_{0.05}[Fe(dmit)_2]$ [105]. Similarly, electrochemical oxidation produced $(n\text{-}Bu_4N)_{0.02}[Fe(dmit)_2]$. Mössbauer studies showed that the Fe atoms are still in the oxidation state (III) and that the coordination number is six. The electrical conductivity of the polycrystalline powders is in the range 10^{-2} to 10^{-1} S cm^{-1} [104,105].

The reaction of $(n\text{-}Bu_4N)[Fe(dmit)_2]$ with $(TTF)_3(BF_4)_2$ affords a black solid, $TTF[Fe(dmit)_2]$, with a conductivity of $\approx 10^{-1}$ S cm^{-1} [105].

Polymers in which pyrazine units link square coplanar $[Fe(dmit)_2]$ units have been reported with a conductivity in the region of 10^{-3} S cm^{-1} [105].

(ii) [Cu(dmit)$_2$] compounds

The preparation of $(n\text{-}Bu_4N)_2[Cu(dmit)_2]$ was described by Steimecke et al. [16]. A series of $[Cu(dmit)_2]$ salts of pyridinium bases has been reported recently [107]. A single crystal X-ray structure of $(epy)_2[Cu(dmit)_2]$ (where epy is *N*-ethylpyridinium) shows that the geometry around copper is greatly distorted from planar with a dihedral angle of 57.3° between the dmit planes. This is most unusual. There are S ··· S contacts between anions (3.613, 3.78 Å) although too weak to form a one-dimensional anion chain but the inter-chain S ··· S contacts are large (4.33 Å). Cyclic voltametry showed $[Cu(dmit)_2]^{2-}$ to be readily oxidized and suspensions of the complex in hexane reacted with I_2 to yield partially oxidized products containing I_3^-.

All the compounds, including the partially oxidized compounds, behaved like semiconductors with low room-temperature conductivities ($<10^{-4}$ S cm^{-1}) [107]. The single crystal ESR spectra of $(n\text{-}Bu_4N)_2[Cu(dmit)_2]$ in the corresponding diamagnetic nickel salt have been studied [108]. The results indicate that the covalency of the metal-to-ligand bond is very high.

(iii) Other bis-chelate dmit compounds

Semiconducting partially oxidized salts of rhodium, $(n\text{-}Bu_4N)_x[Rh(dmit)_2]$ with various stoichiometries ($0.4 < x < 1.5$) as well as iodinated salts, $(n\text{-}Bu_4N)_x[Rh(dmit)_2](I)_y$ ($0.35 < x < 1$; $0.1 < y < 1$) have been described [109]. In addition to the ESR study involving $(n\text{-}Bu_4N)_x[Au/M(dmit)_2]$ [94], a few gold complexes have been extensively studied: these studies concern $(Et_4N)_{0.5}[Au(dmit)_2]$ and $(n\text{-}Bu_4N)_{0.5}[Au(dmit)_2]$ [110] and also long-chain cation compounds, $[Me_m(C_nH_{2n+1})_{4-m}N]_x[Au(dmit)_2]$ used in the preparation of Langmuir–Blodgett films [76,111]. The electrical and spectroscopic properties of bis(dmit)oxomolybdenum complexes and their oxidized analogs have been reported [112] as well as those of similar oxovanadium compounds [113].

(iv) Tris-chelate dmit compounds

$[M(dmit)_3]^{x-}$ complexes have been reported [114]. Attempts to prepare $[Fe(dmit)_3]^{3-}$ and $[Co(dmit)_3]^{3-}$, for which the corresponding mnt complexes are

known (mnt = maleonitriledithiolate), proved unsuccessful. However $[Ph_4As]_3[In(dmit)_3]$, $[Ph_4As][Tl(dmit)_3]$ and $[n\text{-}Bu_4N]_2[V(dmit)_3]$ were successfully prepared. The ESR spectra of the vanadium compound have been studied [114].

G. GENERAL DISCUSSION AND CONCLUSION

The extensive studies of the metal complexes of dmit have arisen because of the understanding that this planar, multi-sulphur-containing ligand would have many advantages over the previously studied dithiolene ligands [12,13,115], in the quest for molecular metals and superconductors based on metal complexes. Since square planar complexes appear to be the most appropriate building blocks for the construction of inorganic molecular conductors, most studies have concentrated on the complexes based on Ni(II), Pd(II) and Pt(II).

(i) The role of the central metal ion

Meaningful comparisons of solid state properties can only be made between compounds possessing the same crystal structure. However, for dmit compounds, precise crystal structure data and solid state properties are not always known for all three members of a particular series of compounds. Therefore, the effect of the central metal ion is difficult to determine. Moreover, the $[M(dmit)_2]$ salts of the same cation possess different crystal structures despite identical methods of synthesis. A good example is the salts of general formula $TTF[M(dmit)_2]_y$. When the central metal is nickel or palladium, $y = 2$, whereas for the Pt complex, $y = 3$ [22]. Even for a given metal, phases with different structures can be obtained: for example, three different phases, α, α', and δ, of the same stoichiometry have been characterized for $TTF[Pd(dmit)_2]_2$. The platinum salt has a different stoichiometry, $TTF[Pt(dmit)_2]_3$, and consequently an entirely different crystal structure [21,22].

Some trends are apparent when all the salts are viewed together. Nickel salts generally form equidistant stack structures at a distance which prevents effective Ni $\cdots$ Ni interactions [20,21,35,54]. Platinum, on the other hand, tends to form structures containing dimers [22]. Not unexpectedly, the palladium salts exhibit intermediate behaviour with the anion forming dimers [82,87,91] and sometimes equidistant stack structures [22]. In this respect, the dmit compounds bear similarities close to those of the more extensively studied mnt complexes.

In contrast to the famous example of KCP [9], in none of the dmit–metal complexes could a direct link be established between metal–metal interaction and high conductivity. However, the nature of the metal atom has been shown to play an indirect, but crucial role in determining the electronic band structure.

For example, some important differences in the temperature–pressure phase diagrams of $TTF[Ni(dmit)_2]_2$ and α'-$TTF[Pd(dmit)_2]_2$ [44,89] have been observed.

The nickel compound remains metallic down to low temperatures whereas the palladium compound undergoes a metal-to-insulator transition. This may be related to the relative position of the Fermi level with respect to the energy of the lowest HOMO band. In the palladium compound, the Fermi level is lower than the lowest HOMO band while in the nickel compound, the Fermi level intersects the top of the lowest HOMO band [43]. Therefore, the palladium compound shows a more pronounced 1D character consistent with the occurrence of a metal-to-insulator transition. In the nickel compound, the Fermi surface exhibits a 2D character; at ambient pressure and low temperatures, the remaining carriers could come from both the TTF bands and the partially filled lowest HOMO band. When applying pressure, the 2D character of the Fermi surface is removed and $TTF[Ni(dmit)_2]_2$ gradually enters the 1D regime and undergoes a metal-to-insulator transition.

The role of the central metal atom is also illustrated by the fact that in $TTF[Ni(dmit)_2]_2$, the superconductive critical temperature T_c increases with increasing pressure whereas in α'-$TTF[Pd(dmit)_2]_2$, T_c decreases with increasing pressure.

The dimerization resulting from a strong Pd ··· Pd interaction in the $Pd(dmit)_2$ slabs of δ-$TTF[Pd(dmit)_2]_2$ and $Cs[Pd(dmit)_2]_2$ induces an inversion of the energies of the antibonding HOMO and bonding LUMO bands; consequently, the partially filled band of these compounds is almost exclusively built from the HOMO of the $Pd(dmit)_2$ acceptor molecules, contrary to intuitive reasoning [43,90]. The unusual physical properties of the equidistantly stacked $TTF[Ni(dmit)_2]_2$ and α'-$TTF[Pd(dmit)_2]_2$ superconducting phases (conductivity studies [44,47], CDW instabilities as evidenced by X-ray scattering studies [48,49], ^1H and ^{13}C NMR studies [31,50,51]) can best be understood if both the HOMO and the LUMO bands of the $M(dmit)_2$ acceptor molecules are partially filled [43,90].

An intermediate situation is encountered in the case of $(Me_4N)[Ni(dmit)_2]_2$: a slight dimerization is observed in the $Ni(dmit)_2$ slabs of this compound. In this case, however, the inter-dimer interactions are not strong enough to change the relative ordering of the dimer energy level and, consequently, the partially filled band is mainly built from the LUMO of the acceptor $Ni(dmit)_2$ molecules [43,90]. This comparison again illustrates the subtle but crucial role of the central metal atom which not only determines the type of stacking but also causes important changes in the band structure, and thus in the physical properties, of apparently very similar inorganic molecular systems.

(ii) The role of the cation

The cation plays a crucial role in determining the packing of the $[M(dmit)_2]$ anions in the crystal structures and hence the physical properties of the salts. In this review we have separated the salts into three categories for convenience. These concerned salts of "open-shell" organic, "closed-shell" organic and inorganic cations.

(a) Salts of "closed-shell" organic cations

The structure and physical properties of these salts are strongly dependent upon the size of the cation and the stoichiometry of the compound. For salts of large cations (e.g. tetrabutylammonium) and a simple stoichiometry, the size of the cation prevents the establishment of close inter-anion interactions. Thus, the compounds do not display interesting solid-state properties and are semi-conducting or insulators. However, non-stochiometric compounds in which the cation-to-anion ratio is low, do possess structures which allow strong interactions between the anions and hence give rise to salts which have reasonably high conductivities at room temperature. For example, the $(n\text{-}Bu_4N)_{0.5}[Pd(dmit)_2]$ and $(n\text{-}Bu_4N)_{0.33}[Pd(dmit)_2]$ salts exhibit metallic conductivity at high temperature, in spite of the size of the $(n\text{-}Bu_4N)$ cation and even though their structures consist of dimers [91]. Recent work on the tetramethylammonium salt $(Me_4N)[Ni(dmit)_2]_2$ has shown, somewhat unexpectedly, that for cations of this size, salts with a cation-to-anion ratio of 1:2 exhibit extensive inter-anion interaction, leading to metallic and even superconducting properties under pressure [54,55].

(b) Salts of "open-shell" organic cations

The combination of TTF and $[Ni(dmit)_2]$ gave rise to the first molecular superconductor containing a metal complex anion [23,24]. Two other superconducting phases, α- and α′-$TTF[Pd(dmit)_2]_2$, based on an "open-shell" organic cation have been reported to date [89], but the corresponding planinum compound, $TTF[Pt(dmit)_2]_3$ does not exhibit superconducting properties. However, compounds containing both cations and anions known to form conducting and superconducting salts would seem to be a fertile avenue for further research in the future.

(c) Salts of inorganic cations

The study of salts of small Group I and Group II cations with $[M(dmit)_2]$ anions has been pursued since the small size of the counter ion should allow strong inter-anion interactions. The studies on the $[M(dmit)_2]$ anions are less extensive than those of the corresponding mnt complexes. Indeed, it has been proved more difficult to prepare the salts of the $[M(dmit)_2]$ compounds despite extensive studies. In both the mnt and dmit series of compounds, the platinum complexes form structures in which the anions are associated as dimer pairs and thus exhibit the properties of semiconductors. In both series of compounds, the nickel complexes form equidistant stack structures, but there are significant differences in the behaviour of the two series of complexes. The larger inter-stack interactions present in the dmit series of compounds are evident from the fact that salts have been prepared in which there is no evidence of a Peierls transition down to 25 mK at ambient pressure, in contrast to the behaviour of the mnt complexes where the nickel salts are all semiconductors.

(iii) Conclusion

In common with the more simple metal bisdithiolene complexes, the conduction process is essentially ligand-centred. The nature of the metal–ligand bonding in the metal bisdithiolenes has been studied by many workers using various computational methods. For the dianions $[Ni(S_2C_2H_2)_2]^{2-}$, the ligand π-orbital combinations are considered to be higher in energy than the appropriate nickel 3d-orbitals. Consequently, the resulting HOMO contains almost entirely ligand orbital character [116,117]. The effect of replacing the two protons by the electron-withdrawing group will be to extend the π system, stabilizing the complex. This would lower the energy of the π orbitals and hence the HOMO should contain more metal orbital character.

The $[M(dmit)_2]$ series of compounds, has produced more than one metallic and superconducting salt. This is a significant improvement on the recently and extensively studied mnt series of compounds [13]. For some of the $[M(dmit)_2]$ compounds discussed in this review, the Peierls distortion has been suppressed, a significant improvement in the synthesis of molecular metals and superconductors over the previously studied tetracyanoplatinate and bis(oxalato)platinate salts, which all exhibit the Peierls instability [118].

One of the most significant characteristics of these compounds is that those which exhibit superconducting behaviour have stoichiometries which are the mirror images of the superconducting TMTSF and BEDT-TTF salts: for example, $(Me_4N)[Ni(dmit)_2]_2$ and $[BEDT\text{-}TTF]_2(I_3)$. The former compounds represent a quarter-filled band system, whereas the organic compounds represent a three-quarter-filled band system. Studies so far show that there are no apparent significant differences in the conducting and superconducting properties of the two series of compounds.

From a chemical point of view, the $M(dmit)_2$ compounds bear some resemblance to the TTF-derived organic molecules. The $M(dmit)_2$ compounds do combine in one molecule the presence of a central metal atom as in KCP and an extended π electron system, but, as discussed above, no direct link could be established between metal–metal interaction and high conductivity. Moreover, the central ethylene (C_2^{4+}) fragment of TTF is isolobal to a (M^{2+}) d^8 metal ion, so that substituting a M^{2+} metal ion for the central double bond of a TTF-based molecule will lead to a $M(bdt)_2$-based complex.

In fact, both these organic and inorganic series were primarily designed by following on the same guidelines for selecting candidate systems which might meet the required structural and electronic criteria for the formation of 1D conductive molecular compounds: (i) 1D stacking of planar molecules; (ii) good orbital overlap between extended π electron systems and/or metal orbitals; (iii) partial filling of the conduction band through either partial oxidation or partial charge transfer between donor and acceptor molecules. Ironically, the first superconductive members of both organic or inorganic series of compounds were shown to exhibit interstack interactions that make them no longer 1D but rather quasi-1D or even 2D. Even more

ironically, in the so-called κ-type structure of the molecular superconductors with the highest T_c, for example (BEDT-TTF)$_2$Cu(NCS)$_2$ [6], the BEDT-TTF donor molecule packing motifs are no longer 1D but instead consist of orthogonally arranged dimers. The electronic bandwidths and the shapes of the Fermi surface depending heavily on the packing arrangement, it would therefore be presumptuous at this point to attempt a detailed comparison of conduction mechanisms in the organic and in the inorganic compounds. We shall therefore restrict ourselves to listing the conspicuous differences in the conduction mechanism in both series of conductors, especially the superconductors:

(a) In all organic superconductors, the superconductive critical temperature T_c decreases with increasing pressure. In $(Me_4N)[Ni(dmit)_2]_2$ and $TTF[Ni(dmit)_2]_2$, T_c varies in opposite ways with increasing pressure.

(b) The low-pressure metal-to-insulator transitions observed in $TTF[Ni(dmit)_2]_2$ and α'-$TTF[Pd(dmit)_2]_2$ involve a CDW state, instead of SDW or spin-Peierls state as for the purely organic superconductors.

(c) $TTF[Ni(dmit)_2]_2$ is the first molecular superconductor in which a CDW instability does not induce a metal-to-insulator transition.

(d) The electronic band structure calculations of $M(dmit)_2$ systems reveal a unique "multi-band Fermi surface" situation.

All these findings indicate that the electrical properties of the dmit-based superconductors exhibit novel features.

The results detailed in this review may point the way to the preparation of new compounds with new or improved solid state properties. In particular, we may anticipate the preparation of compounds having higher electrical conductivities at room temperature, more compounds which retain their metallic properties down to very low temperatures and the preparation of new superconductors with higher transition temperatures.

ACKNOWLEDGEMENTS

Thanks are due to the contributions of the co-authors indicated in the citations. P.C. and L.V., are indebted to Professor J.-P. Legros for X-ray diffraction structure analysis and useful discussions, and to other contributors, particularly L. Brossard (University of Orsay) for his major involvement in physical measurements. H.K. and A.K. gratefully thank Professor R. Kato (ISSP, Tokyo) for his collaboration. A.E.U. and R.A.C. gratefully acknowledge the contribution of R. Friend.

REFERENCES

1 A. Mueller, Polyhedron, 5 (1986) 323.
2 G. Wilkinson, R.D. Gillard and J.A. McCleverty (Eds.), Comprehensive Coordination Chemistry, Vol. 6, Pergamon Press, New York, 1987, pp. 541–1027.

3 R.H. Holm, Acc. Chem. Res., 10 (1977) 427.
4 J.R. Ferraro and J.M. Williams, Introduction to Synthetic Electrical Conductors, Academic Press, New York, 1987, pp. 1–327.
5 M. Aldissi (Ed.), Proceedings of the International Conference on Science and Technology of Synthetic Metals, Synth. Met. 17 (1988) A1–A528, B1–B666; 28 (1989) C1–C886, D1–D740, 29 (1989) E1–E774, F1–F752.
6 G. Saito and S. Kagoshima (Eds.), The Physics and Chemistry of Organic Superconductors, Springer Proceedings in Physics, Vol. 51, Springer Verlag, Berlin, 1990, pp. 1–476.
7 W. Knop and G. Schnedermann, J. Prakt. Chem., 37 (1846) 461.
8 K. Krogmann, Angew. Chem. Int. Ed. Engl., 8 (1969) 35 and references cited therein.
9 H.R. Zeller, Festkoerperprobleme, 13 (1973) 31.
10 (a) J.M. Williams, A.J. Schultz, A.E. Underhill and K. Carneiro, in J.S. Miller (Ed.), Extended Linear Chain Compounds, Vol. 1, Plenum Press, New York, 1982, pp. 73–118.
(b) A.E. Underhill, D.M. Watkins, J.M. Williams and K. Carneiro, in J. S. Miller (Ed.), Extended Linear Chain Compounds, Vol. 1, Plenum Press, New York, 1982, pp. 119–156.
11 (a) L.B. Coleman, M.J. Cohen, D.J. Sandman, F.G. Yamagishi, A.F. Garito and A.J. Ferraris, Solid State Commun., 12 (1973) 1125.
(b) J.P. Ferraris, D.O. Cowan, V. Valatka and J.H. Perlstein, J. Am. Chem. Soc., 95 (1973) 948.
12 (a) K.W. Browal and L.V. Interrante, J. Coord. Chem., 3 (1973) 27.
(b) L. Alcacer and H. Novais, in J.S. Miller (Ed.), Extended Linear Chain Compounds, Vol. 3, Plenum Press, New York, 1983, pp. 319–351.
13 (a) M.M. Ahmad, D.J. Turner, A.E. Underhill, C.S. Jacobsen, K. Mortensen and K. Carneiro, Phys. Rev. B, 29 (1984) 4796.
(b) P.I. Clemenson, PhD Thesis, University of Wales, 1987.
14 R.E. Peierls, Quantum Theory of Solids, Clarendon Press, Oxford, 1955.
15 (a) F. Wudl, J. Am. Chem. Soc., 103 (1981) 7064.
(b) F. Wudl, Pure Appl. Chem., 54 (1982) 1051.
16 G. Steimecke, R. Kirmse and E. Hoyer, Z. Chem., 15 (1975) 28.
17 G. Steimecke, H.J. Sieler, R. Kirmse and E. Hoyer, Phosphorus and Sulphur, 7 (1979) 49.
18 (a) J.B. Torrance, Acc. Chem. Res., 11 (1979) 79.
(b) J.B. Torrance, in W.E. Hatfield (Ed.), Molecular Metals, Vol. 1, NATO Conferences Series, Series VI, Plenum Press, New York, 1979, pp. 7–23.
19 K.S. Varma, A. Bury, N.J. Harris and A.E. Underhill, Synthesis, (1987) 837.
20 (a) L. Valade, M. Bousseau, A. Gleizes and P. Cassoux, J. Chem. Soc. Chem. Commun., (1983), 110.
(b) L. Valade, J.-P. Legros, M. Bousseau, P. Cassoux, M. Garbauskas and L.V. Interrante, J. Chem. Soc. Dalton Trans., (1985) 783.
21 M. Bousseau, L. Valade, M.-F. Bruniquel, P. Cassoux, M. Garbauskas, L.V. Interrante and J. Kasper, Nouv. J. Chim., 8 (1984) 3.
22 M. Bousseau, L. Valade, J.-P. Legros, P. Cassoux, M. Garbauskas and L.V. Interrante, J. Am. Chem. Soc., 108 (1986) 1908.
23 (a) L. Brossard, M. Ribault, M. Bousseau, L. Valade and P. Cassoux, C.R. Acad. Sci. Ser. II, 302 (1986) 205.
(b) J. Friedel and F. Gallais, C.R. Acad. Sci. Ser. Gen. Vie Sci., 3 (1988) 181.
24 L. Brossard, M. Ribault, L. Valade and P. Cassoux, Physica B & C (Amsterdam), 143 (1986) 378.
25 A. Kobayashi, H. Kim, Y. Sasaki, R. Kato and H. Kobayashi, Solid State Commun., 62 (1987) 57.

26 (a) G.C. Papavassiliou, Z. Naturforsch. Teil B, 36 (1981) 1200.
(b) G.C. Papavassiliou, J. Phys. (Paris), 44 (1983) 1257.
27 D. Zhu, M. Wang, P. Wang, D. Wang and S. Liu, Kexue Tongbao, 31 (1986) 382,
28 J. Ribas and P. Cassoux, C.R. Acad. Sci. Ser. II, 293 (1981) 287.
29 J.-P. Ulmet, P. Auban, A. Khmou, L. Valade and P. Cassoux, Phys. Lett. A, 113 (1985) 217.
30 J.E. Schirber, D.L. Overmyer, J.M. Williams, H.H. Wang, L. Valade and P. Cassoux, Phys. Lett. A, 120 (1987) 87.
31 C. Bourbonnais, P. Wzietek, D. Jérome, F. Creuzet, L. Valade and P. Cassoux, Europhys. Lett., 6 (1988) 177.
32 L. Brossard, M. Ribault, L. Valade and P. Cassoux, C.R. Acad. Sci. Ser. II, 309 (1989) 1117.
33 (a) I. Johansen, K. Bechgaard, C. Rindorf, N. Thorup, C.S. Jacobsen and K. Mortensen, Synth. Met., 15 (1986) 333.
(b) K. Bechgaard, Stud. Org. Chem. (Amsterdam), 25 (1986) 391.
34 (a) R. Kato, H. Kobayashi, A. Kobayashi, T. Naito, M. Tamura, H. Tajima and H. Kuroda, Chem. Lett., (1989) 1839.
(b) A. Kobayashi, R. Kato and H. Kobayashi, in G. Saito and S. Kagoshima (Eds.), The Physics and Chemistry of Organic Superconductors, Vol. 51, Springer Verlag, Berlin, 1990, pp. 32–35.
(c) S. Kagoshima, personal communication, 1990.
35 R. Kato, H. Kobayashi, A. Kobayashi and Y. Sasaki, Chem. Lett., (1985) 131.
36 (a) H. Kobayashi, R. Kato, T. Mori, A. Kobayashi and Y. Sasaki, Mol. Cryst. Liq. Cryst., 125 (1985) 125.
(b) A. Kobayashi, R. Kato and H. Kobayashi, Synth. Met., 19 (1987) 635.
37 L. Valade and P. Cassoux, C.R. Acad. Sc. Ser. II, 301 (1985) 999.
38 H. Kobayashi, R. Kato, A. Kobayashi and Y. Sasaki, Chem. Lett., (1985) 535.
39 A. Kobayashi, R. Kato, H. Kobayashi, T. Mori and H. Inokuchi, Physica B & C (Amsterdam), 143 (1986) 562.
40 H. Kobayashi, R. Kato, A. Kobayashi and Y. Sasaki, Chem. Lett., (1985) 191.
41 H. Strzelecka, R. Vicente, J. Ribas, J.-P. Legros, P. Cassoux, P. Petit and J.-J. André, Polyhedron, 10 (1991) 687.
42 Y. Sakamoto, G. Matsubayashi and T. Tanaka, Inorg. Chim. Acta, 113 (1986) 137.
43 (a) E. Canadell, E.I. Rachidi, S. Ravy, J.-P. Pouget, L. Brossard and J.-P. Legros, J. Phys. (Paris), 50 (1989) 2967.
(b) E. Canadell, S. Ravy, J.-P. Pouget and L. Brossard, Solid State Commun., 75 (1990) 633.
44 L. Brossard, M. Ribault, L. Valade and P. Cassoux, Phys. Rev. B, 42 (1990) 3935.
45 D. Jérome and H.J. Schulz, Adv. Phys., 31 (1982) 299.
46 J.E. Schirber, L.J. Azevedo, J.F. Kwak, E.L. Venturini, P.C.W. Leung, M.A. Beno, H.H. Wang and J.M. Williams, Phys. Rev., 33 (1986) 1987.
47 P. Cassoux, L. Valade, J.-P. Legros, C. Tejel, J.-P. Ulmet and L. Brossard, in G. Saito and S. Kagoshima (Eds.), The Physics and Chemistry of Organic Superconductors, Vol. 51, Springer Verlag, Berlin, 1990, pp. 22–27.
48 S. Ravy, J.-P. Pouget, L. Valade and J.-P. Legros, Europhys. Lett., 9 (1989) 391.
49 S. Ravy, E. Canadell and J.-P. Pouget, in G. Saito and S. Kagoshima (Eds.), The Physics and Chemistry of Organic Superconductors, Vol. 51, Springer Verlag, Berlin, 1990, pp. 252–256.
50 A. Vainrub, D. Jérome, M.-F. Bruniquel and P. Cassoux, Europhys. Lett., 12 (1990) 267.

51 A. Vainrub, E. Canadell, D. Jérome, P. Bernier, T. Nunes, M.-F. Bruniquel and P. Cassoux, J. Phys. (Paris), 51 (1990) 2465.
52 W. Kang, PhD Thesis, Université de Paris Sud, Orsay, 1989.
53 L.R. Groeneveld, PhD Thesis, Leiden, 1988.
54 H. Kim, A. Kobayashi, Y. Sasaki, R. Kato and H. Kobayashi, Chem. Lett., (1987) 1799.
55 (a) A. Kobayashi, H. Kim, Y. Sasaki, R. Kato, H. Kobayashi, S. Moriyama, Y. Nishio, K. Kajita and W. Sasaki, Chem. Lett., (1987) 1819.
(b) A. Kobayashi, H. Kim, Y. Sasaki, S. Moriyama, Y. Nishio, K. Kajita, W. Sasaki, R. Kato and H. Kobayashi, Synth. Met., 27 (1988) B339.
56 (a) K. Kajita, Y. Nishio, S. Moriyama, R. Kato, H. Kobayashi and W. Sasaki, Solid State Commun., 65 (1988) 361.
(b) H. Kobayashi, R. Kato, A. Kobayashi, T. Mori, H. Inokuchi, Y. Nishio, K. Kajita and W. Sasaki, Synth. Met., 27 (1988) A289.
57 (a) H. Tajima, M. Tamura, T. Naito, A. Kobayashi, R.A., Clark and A.E. Underhill, Mol. Cryst. Liq. Cryst., 181 (1990) 233.
(b) H. Tajima, T. Naito, M. Tamura, A. Takahashi, S. Toyoda, A. Korbayashi, H. Kuroda, R. Kato, H. Kobayashi, R.A. Clark and A.E. Underhill, Synth. Met., 42 (1991) 2417.
58 (a) L.R. Groeneveld, B. Schuller, G.J. Kramer, J.G. Haasnoot and J. Reedijk, Rec. Trav. Chim. Pays-Bas, 105 (1986) 507.
(b) L.R. Groeneveld, G.J. Kramer, T.B.L.W. von Marinelli, H.B. Brom, J.G. Haasnoot and J. Reedijk, in P. Delhaes and M. Drillon (Eds.), Organic and Inorganic Low-Dimensional Crystalline Materials, Plenum Press, New York, 1987, pp. 349–352.
59 J. Kisch, J. Bücheler, A. Fernandez, H. Görner and N. Zeug, Sci. Pap. Inst. Phys. Chem. Res. Jpn., 78 (1984) 178.
60 (a) G.J. Kramer, L.R. Groeneveld, J.L. Joppe, H.B. Brom, L.J. de Jongh and J. Reedijk, Synth. Met., 19 (1987) 745.
(b) G.J. Kramer and H.B. Brom, Synth. Met., 27 (1988) A133.
61 G.J. Kramer, J.C. Jol, H.B. Brom, L.R. Groeneveld and J. Reedijk, J. Phys. C, 21 (1988) 4591.
62 G.J. Kramer and H.B. Brom, J. Phys. C, 21 (1988) 6085.
63 R. Kato, T. Mori, A. Kobayashi, Y. Sasaki and H. Kobayashi, Chem. Lett., (1984) 1.
64 O. Lindqvist, L. Sjolin, J. Sieler, G. Steimecke and E. Hoyer, Acta. Chim. Scand. Ser. A, 33 (1979) 445.
65 O. Lindqvist, L. Andersen, J. Sieler, G. Steimecke and E. Hoyer, Acta Chim. Scand. Ser. A, 36 (1982) 855.
66 D. Mentzafos, A. Hountas and A. Terzis, Acta Crystallogr. Sect. C, 44 (1988) 1550.
67 R. Kato, H. Kobayashi, H. Kim, A. Kobayashi, Y. Sasaki, T. Mori and H. Inokuchi, Chem. Lett., (1988) 865.
68 R. Kato, H. Kobayashi, H. Kim, A. Kobayashi, Y. Sasaki, T. Mori and H. Inokuchi, Synth. Met., 27 (1988) B359.
69 L. Valade, J.-P. Legros, C. Tejel, B. Pomarède, B. Garreau, M.-F. Bruniquel, P. Cassoux, J.-P. Ulmet, A. Audouard and L. Brossard, Synth. Met., 42 (1991) 2268.
70 C. Tejel, B. Pomarede, J.-P. Legros, L. Valade, P. Cassoux and J.-P. Ulmet, Chem. Mater., 1 (1989) 578.
71 J.-P. Ulmet, M. Mazzaschi, C. Tejel, P. Cassoux and L. Brossard, Solid State Commun., 74 (1990) 91.
72 A. Isuoka, A. Miyazaki, N. Sato, T. Sugawara and T. Enoki, in G. Saito and S. Kagoshima (Eds.), The Physics and Chemistry of Organic Superconductors, Vol. 51, Springer Verlag, Berlin, 1990, pp. 32–35.

73 R.A. Clark, A.E. Underhill, R. Friend, M. Allen, I. Marsden, A. Kobayashi and H. Kobayashi, in G. Saito and S. Kagoshima (Eds.), The Physics and Chemistry of Organic Superconductors, Vol. 51, Springer Verlag, Berlin, 1990, pp. 28–31.
74 L. Valade, J.-P. Legros, P. Cassoux and F. Kubel, Mol. Cryst. Liq. Cryst., 140 (1986) 335.
75 T. Nakamura, H. Tanaka, M. Matsumoto, H. Tachinaba, E. Manda and Y. Kawabata, Chem. Lett., (1988) 1667.
76 T. Nakamura, H. Tanaka, M. Matsumoto, H. Tachinaba, E. Manda and Y. Kawabata, Synth. Met., 27 (1988) B601.
77 G.C. Papavassiliou, Z. Naturforsch. Teil B, 37 (1982) 825.
78 G.C. Papavassiliou, A.M. Cotsilios and C.S. Jacobsen, J. Mol. Struct., 115 (1984) 41.
79 L. Valade, P. Cassoux, A. Gleizes and L.V. Interrante, J. Phys. Colloq., 44C3 (1983) 1183.
80 G.C. Papavassiliou, Mol. Cryst. Liq. Cryst., 86 (1982) 159.
81 R.A. Clark, PhD Thesis, University of Wales, 1989.
82 R.A. Clark and A.E. Underhill, J. Chem. Soc. Chem. Commun., (1989) 228.
83 A. Kobayashi and H. Kobayashi, unpublished results.
84 R. Friend, I. Parker and I. Marsden, personal communication, 1990.
85 P. Cassoux, L. Valade, J.-P. Legros, L. Interrante and C. Roucau, Physica B & C (Amsterdam), 143 (1986) 313.
86 L. Valade, M. Bousseau and P. Cassoux, Nouv. J. Chim., 9 (1985) 351.
87 J.-P. Legros and L. Valade, Solid State Commun., 68 (1988) 599.
88 L. Brossard, H. Hurdequint, M. Ribault, L. Valade, J.-P. Legros and P. Cassoux, Synth. Met., 27 (1988) B157.
89 L. Brossard, M. Ribault, L. Valade and P. Cassoux, J. Phys. (Paris), 50 (1989) 1521.
90 L. Brossard, E. Canadell, S. Ravy, J.-P. Pouget, J.-P. Legros and L. Valade, Fizika, 21 (1989) 15.
91 J.-P. Legros, L. Valade and P. Cassoux, Synth. Met., 27 (1988) B347.
92 G.J. Kramer, PhD Thesis, Leiden, 1988.
93 G.C. Papavassiliou, G. Mousdis, V. Kakoussis, A. Terzis, A. Hountas, B. Hilti, C.W. Mayer and J.S. Zambounis, in G. Saito and S. Kagoshima (Eds.), The Physics and Chemistry of Organic Superconductors, Vol. 51, Springer Verlag, Berlin, 1990, pp. 247–250.
94 R. Kirmse, J. Stach, W. Dietzsch, G. Steimecke and E. Hoyer, Inorg. Chem., 19 (1980) 2679.
95 R. Vicente, J. Ribas, X. Solans, M. Font-Altaba, A. Mari, Ph. de Loth and P. Cassoux, Inorg. Chim. Acta, 132 (1987) 229.
96 A. Kobayashi, H. Kim, Y. Sasaki, K. Murata, R. Kato and H. Kobayashi, J. Chem. Soc. Faraday Trans., 86 (1990) 361.
97 A. Kobayashi and H. Kobayashi, unpublished results.
98 R.A. Clark and A.E. Underhill, Synth. Met. 27 (1988) B515.
99 A.E. Underhill, R.A. Clark, I. Marsden, M. Allen, R.H. Friend, H. Tajima, T. Naito, M. Tamura, H. Kuroda, A. Kobayashi, H. Kobayashi, E. Canadell, S. Ravy and J.-P. Pouget, J. Phys. C., 3 (1991) 933.
100 A. Kobayashi, Y. Sasaki, R. Kato and H. Kobayashi, Chem. Lett., (1986) 387.
101 A. Kobayashi, H. Kobayashi, R.A. Clark and A.E. Underhill, unpublished results.
102 V.N. Baumer, V.A. Starodub and G.E. Tarasova, Sov. Phys. Crystallogr., 34 (1989) 59.
103 A. Kobayashi and H. Kobayashi, unpublished results.
104 F. Kubel, L. Valade, J. Strähle and P. Cassoux, C.R. Acad. Sci. Ser. II, 295 (1982) 179.
105 F. Kubel, J. Strähle and P. Cassoux, J. Phys. Colloq., 44C3 (1983) 1265.
106 H. Poleschner, E. Fanghänel and H. Mehner, J. Prakt. Chem., 323 (1981) 919.
107 G. Matsubayashi, K. Takahashi and T. Tanaka, J. Chem. Soc. Dalton Trans., (1988) 967.

108 J. Stach, R. Kirmse, W. Dietzsch, R.M. Olk and E. Hoyer, Inorg. Chem., 23 (1984) 4779.
109 K. Yokoyama, G.E. Matsubayashi and T. Tanaka, Polyhedron, 7 (1988) 379.
110 A.V. Zvarykina, A.I. Kotov, V.N. Laukhin, M.K. Maskova, V.N. Merzhanov, S.S. Nagapetyan, Yu. T. Struchkov, L. Yu. Ukhin, V.E. Shkolver and E.B. Yagubskii, International Conference on Electronics of Organic Metals, Tashkent, 1987, Paper A-20.
111 T. Nakamura, Y. Miura, M. Matsumoto, H. Tashinaba, M. Tanaka and Y. Kawabata, in G. Saito and S. Kagoshima (Eds.), The Physics and Chemistry of Organic Superconductors, Vol. 51, Springer Verlag, Berlin, 1990, pp. 424–427.
112 T. Nojo, G. Matsubayashi and T. Tanaka, Inorg. Chim. Acta, 159 (1989) 49.
113 G. Matsubayashi, K. Akika and T. Tanaka, Inorg. Chem., 27 (1988) 4744.
114 R.M. Olk, W. Dietzsch, R. Kirmse, J. Stach, E. Hoyer and L. Golic, Inorg. Chim. Acta, 128 (1987) 251.
115 (a) J.A. McCleverty, Prog. Inorg. Chem., 10 (1968) 49.
(b) R. Eisenberg, Prog. Inorg. Chem., 12 (1970) 295.
(c) P.I. Clemenson, Coord. Chem. Rev., 106 (1990) 171.
(d) E. Hoyer, W. Dietzsch and W. Schroth, Z. Chem., 11 (1971) 41.
(e) J.A. McCleverty, in C.C. Addison and D.B. Sowerby (Eds.), MTP International Review of Science, Inorganic Chemistry, Series 1, Vol. 2, Butterworths, London, 1972, pp. 301–327.
116 M.R.A. Blomberg and V. Whalgren, Chem. Phys., 49 (1980) 117.
117 I. Fischer-Hjalmars and A. Henricksson-Enflow, Quantum Chem. Symp., 16 (1982) 1.
118 A.F. Underhill and D.M. Watkins, Chem. Soc. Rev., 9 (1980) 429.